DIPLOMARBEIT

On the Generation of Minimal Surfaces

ausgeführt am

Institut für
Diskrete Mathematik und Geometrie
TU Wien

unter der Anleitung von

Prof. Dr.techn. Christian Müller

durch

Cornelia Michlits, BSc.

Cornelia Michlits	Christian Müller

Wien, am February 16, 2023

Kurzfassung

Minimalflächen, die durch das Verschwinden ihrer mittleren Krümmung charakterisiert sind, haben Mathematiker/-innen aufgrund ihrer geometrischen Aspekte sowie als variationelles Problem oder aus der Sicht der partiellen Differentialgleichungen, seit Mitte des 18. Jhd. fasziniert. Sie finden auch außerhalb der Mathematik zahlreiche Anwendungen, beispielsweise im 3D-Druck zur Erzeugung von stabilen Objekten mit geringem Gewicht, in den Materialwissenschaften, der Physik und wegen ihrer ästhetischen Erscheinung auch in der Architektur. In dieser Arbeit stellen wir einen neuartigen Ansatz vor, um aus drei bekannten Minimalflächen, welche nicht alle der gleichen assoziierten Familie angehören, neue Flächen zu erzeugen, die in jeder Polstellen-freien Umgebung, Minimalflächen darstellen. Dazu identifizieren wir holomorphe, isotrope Funktionen, sogenannte Minimalkurven, mit Punkten auf einer projektiven Quadrik und bilden den Kegelschnitt mit der Ebene bestehend aus drei paarweise verschiedenen Minimalkurven. Im Fall von algebraischen Minimalflächen ist die resultierende Funktion meromorph und der Weierstraßsche Darstellungssatz kann angewendet werden. Wir verifizieren Minimalflächen aus derselben assoziierten Familie als Erzeugende auf der Quadrik, die ein Kegel ist. Zahlreiche so erhaltene Flächen werden visualisiert sowie auch die Verformungen der Minimalflächen entlang des Kegelschnitts. Weiters verwenden wir die Christoffel Dualität und Möbiustransformation, um weitere Minimalflächen für unseren Algorithmus zu erhalten. Zusätzlich, wird ein 3D Model einer generierten Fläche erzeugt und gedruckt.

Abstract

Minimal surfaces, characterized as those with vanishing mean curvature, fascinate mathematicians since the mid-18th century due to their geometric properties, as a problem of calculus of variations or of partial differential equations. Their multifaceted applications are not restricted to mathematics, but also extend to 3D printing for the production of lightweight structures, to material science as well as physics and, due to their aesthetic appearance, also to architecture. In this thesis we present a novel approach to generate surfaces from three known minimal surfaces not belonging to the same associated family, which represent, locally in a pole-free neighborhood, minimal surfaces themselves. For this purpose, we identify minimal curves as points on a projective quadric and build the conic section with the plane spanned by three pairwise different minimal curves. In the case of three algebraic minimal surfaces, the resulting minimal curve is meromorphic and we can make use of the Weierstrass representation theorem. We verify minimal surfaces of an associated family as the rulings on the quadric, which is a cone. Several surfaces obtained via this construction are visualized as well as the deformation of minimal surfaces, like Enneper's surfaces, along the conic section. Further, we use the Christoffel dual and Möbius transformation to obtain further surfaces and use them as initial minimal curves in our algorithm. Additionally, a 3D model of a generated surface is created and printed.

Eidesstattliche Erklärung

Ich erkläre an Eides statt, dass ich die vorliegende Diplomarbeit selbstständig und ohne fremde Hilfe verfasst, andere als die angegebenen Quellen und Hilfsmittel nicht benutzt bzw. die wörtlich oder sinngemäß entnommenen Stellen als solche kenntlich gemacht habe.

Wien, am February 16, 2023

Cornelia Michlits

Contents

1 Introduction

The first discovered minimal surface, i.e., a regular surface with vanishing mean curvature, was the catenoid. Euler provided, in the middle of the 18th century, a proof that the catenoid minimizes locally at each point the surface area [Eul52, GAS17]. Retrospectively, this, and the partial differential equation, that a minimal surface needs to satisfy, formulated by Lagrange approximately at the same time, represents the starting point of the theory of minimal surfaces [Lag60, GAS17]. Later, Meusnier [Meu85] identified the helicoid as a minimal surface, which is, beside the plane, the only ruled minimal surface, i.e., for every point on the surface there is a straight line through that point that is entirely contained in the surface [DC86]. There were no other examples known for decades, until Scherk used a version of Lagrange's equation modified by Monge as well as separation of variables in order to generate further examples, known as the Scherk's surfaces [Nit89]. Though the problem of finding a minimal surface, given a simply closed boundary curve, can be traced back to Euler and Lagrange, it is famously known as Plateau's problem, named after a physicist who experimented with soap films and thereby popularized it. By dipping wire loops into soapy water, he experimentally generated some instances of minimal surfaces and thus showed that these structures occur in nature [EJ14].

Nowadays, several practical application are known, for example block copolymers in material science form minimal surfaces [LM83; AH+84; SKO20]. The gyroid, an infinite surface that is periodic in three independent directions, found by Schoen in 1970 [Sch70] is used in 3D printing applications to produce lightweight components. Due to aesthetic reasons minimal surfaces also inspire modern architecture [Emm13]. [Nit89] further lists theory of elasticity and fluid dynamics as examples.

From a mathematical point of view, the existence of a minimal surface for a given closed boundary curve without self-intersections, was unknown for several decades [EJ14]. First existence proofs were found in the 1930s independently by Douglas and Radó [Dou31; Rad30]. A proof by Courant [Cou37; EJ14], is provided in Chapter 3. Essential insights on their generation, however, were gained earlier by Weierstrass, who found a relation of minimal surfaces and holomorphic isotropic functions and additionally, stated a formula for their generation [Wei66]. This theorem is of further interest for our investigations and can be found in Chapter 4. Another way to generate minimal surfaces can be traced back to Lie [Nit89], who considered them as translation surfaces, i.e., a surface obtained by translation of a curve along another one, of an isotropic curve and its complex conjugated curve. Odehnal lists these as some of the rarely known results for generating algebraic minimal surfaces [Ode16].

In this work we deal with the following questions:

- Can we generate a new minimal surface from known ones, e.g., Enneper's minimal surfaces, via identification of minimal curves as points on a projective quadric?
- Is it feasible to parameterize the intersection of this cone with the plane spanned by three pairwise different minimal surfaces?
- Under which condition is the newly obtained function a minimal surface?
- What statements can be derived via this construction for the associated family of minimal surfaces?
- How do visualizations of the so generated surfaces look like?

These issues are mainly covered in Chapter 6. Chapter 7 considers integrands containing analytic functions and the associated challenges to calculate the path integral in Weierstrass theorem. Furthermore, we utilize minimal surfaces, obtained by the Christoffel dual and Möbius transformations, as initial functions in order to calculate the conic section with a plane spanned by these points Chapter 8.

2 Preliminaries

2.1 Differential Geometry and Mean Curvature

First, some terms and concepts from differential geometry are repeated. Particular attention is paid to the concept of mean curvature, which is used to define minimal surfaces.

Definition 1. *A **(local) surface** is a differentiable mapping $x : \mathcal{U} \to \mathbb{R}^n$, where $\mathcal{U} \subseteq \mathbb{R}^2$ is open. Let $J(x)(u,v)$ denote the Jacobian of x at (u,v). If $\det(J(x)(u,v)) \neq 0$ for all $(u,v) \in \mathcal{U}$, the surface x is called **regular** [GAS17, Ch. 10.1].*

Definition 2. *Let $\mathcal{M}$ be a regular surface and u, v tangent vectors in the tangential space $T_p\mathcal{M}$ at p. The inner product $I_p(u,v) := \langle u, v\rangle$ is called the **first fundamental form**. Let further N denote the unit normal vector field. The linear map $S : T_p\mathcal{M} \to T_p\mathcal{M}, v \mapsto D_vN$ denotes the **shape operator** and $II_p(u,v) := \langle S(u), v\rangle$ is the **second fundamental form** [GAS17, Ch. 13.4].*

The first fundamental form defines a positive definite symmetric bilinear form. The shape operator is self-adjoint endomorphism and hence, diagonalizable with real eigenvalues [EJ14, p.49].

Definition 3. *The eigenvalues $\kappa_1(p), ..., \kappa_m(p)$ of the shape operator $S : T_p\mathcal{M} \to T_p\mathcal{M}$ are called the **principal curvatures** [GAS17, Ch. 13.3].*

Definition 4. *The functions $H, K : \mathcal{M} \to \mathbb{R}$*

$$\begin{aligned} H(p) &= \frac{1}{m}\operatorname{tr}(S(p)) \\ K(p) &= \det(S(p)) \end{aligned}$$

*denote the **mean** and **Gaussian curvature**, respectively [GAS17, Ch. 13.4].*

Choosing an orthonormal eigenbasis of the shape operator S yields a diagonal matrix with $diag(S) = (\kappa_1, \ldots, \kappa_m)$ and therefore, the following relationship between the mean, Gaussian and principal curvature can be derived [GAS17, Ch. 13.4].

Proposition 1. *Let $H(p), K(p)$ denote the mean and Gaussian curvature, respectively. Then one has*

$$\begin{aligned} H(p) &= \frac{1}{m}(\kappa_1 + ... + \kappa_m) \\ K(p) &= \kappa_1 \cdot \cdots \cdot \kappa_m. \end{aligned}$$

Lemma 1. *Let $x : \mathcal{U} \to \mathbb{R}^3$ be a regular surface. Then $\{x_u, x_v\}$ form a basis of the tangential space $T_p\mathcal{M}$, $T_p\mathcal{M} \ni t = ax_u + bx_v$ for $a, b \in \mathbb{R}$ and the first and second fundamental form is given by the following equations*

$$I_p(t,t) = Ea^2 + 2Fab + Gb^2 \tag{2.1}$$
$$II_p(t,t) = ea^2 + 2fab + gb^2 \tag{2.2}$$

where

$$E = \langle x_u, x_u \rangle, F = \langle x_u, x_v \rangle \text{ and } G = \langle x_v, x_v \rangle \tag{2.3}$$
$$e = \langle N, x_{uu} \rangle, f = \langle N, x_{uv} \rangle \text{ and } g = \langle N, x_{vv} \rangle, \tag{2.4}$$

are the coefficients of the first and second fundamental form, respectively [GAS17, Ch. 13.4].

Depending on the convention, sometimes the equations (2.4) are used with a negative sign.

Lemma 2. *For a regular surface $x : \mathcal{U} \to \mathbb{R}^3$ the mean curvature can be expressed by*

$$H = \frac{eG - 2fF + gE}{2(EG - F^2)}.$$

Proof. See for example [GAS17, Ch. 13.4]. □

Definition 5. *Let $\mathcal{U}$ be an open subset of $\mathbb{C}$. A function $\psi : \mathcal{U} \to \mathbb{R}^n$ is a **conformal parametrization**, if*

$$\langle \psi_u, \psi_v \rangle = 0 \text{ and } ||\psi_u|| = ||\psi_v|| \tag{2.5}$$

holds [GAS17, Ch. 16.7; EJ14, Ch. 8.4].

Remark: For a conformal parameterized mapping, the mean curvature simplifies to

$$H = \frac{e+g}{2E}. \tag{2.6}$$

Definition 6. *A regular surface $\mathcal{M}$ is called **minimal surface**, if the mean curvature vanishes for every point on $\mathcal{M}$ [GAS17, Ch. 13.4; EJ14, Ch. 8.1].*

Example 1. *The **catenoid** (see Figure 2.1a)*

$$cat(u,v) = \left(c\cos u \cosh \frac{v}{c}, c \sin u \cosh\left(\frac{v}{c}\right), v\right), \tag{2.7}$$

with $c \in \mathbb{R}\backslash\{0\}$, has principal curvature $\kappa_1 = -\kappa_2$ and hence, zero mean curvature [GAS17, Ch. 15.1].

Example 2. *The **helicoid** (see Figure 2.1b) is a minimal surface [GAS17, Ch. 12.5] parameterized by*

$$hel(u,v) = (v\cos(u), v\sin(u), u). \tag{2.8}$$

(a) Catenoid (b) Helicoid

Figure 2.1: Examples of minimal surfaces.

Theorem 1. *There is a deformation between a catenoid and a helicoid, given by the following formula*

$$z_t(u,v) = \cos(t)\left(\sinh(v)\sin(u), -\sinh(v)\cos(u), u\right) + \sin(t)\left(\cosh(v)\cos(u), \cosh(v)\sin(u), v\right), \quad (2.9)$$

where $z_0(u,v)$ defines a helicoid and $z_{\frac{\pi}{2}}(u,v)$ a catenoid. Moreover, for all parameter values t the resulting surface is minimal and locally isometric to z_0 [GAS17, Ch. 16].

A visualization of the deformation is presented in Figure 2.2.

2.2 Complex Analysis

Based on [Jän13] we recap isolated singularities and their different types as well as meromorphic functions.

Definition 7. *Let $\mathcal{U} \subseteq \mathbb{C}$ be open and $f : \mathcal{U} \to \mathbb{C}$ be a holomorphic function. Isolated points of $\mathbb{C} \setminus \mathcal{U}$ are called isolated singularities.*

Definition 8. *An isolated singularity z_0 of $f : \mathcal{U} \to \mathbb{C}$ is called*

1. ***removable**, if f can be extended to a holomorphic function $\tilde{f} : \mathcal{U} \cup \{z_0\} \to \mathbb{C}$*
2. ***pole**, if z_0 is not removable and there is an $m \geq 1$ such that $(z - z_0)^m f(z)$ is removable at z_0*
3. ***essential**, if z_0 is neither removable nor a pole.*

The smallest possible m in (2) is denoted as the order of the pole.

Definition 9. *A function $\psi : \mathcal{U} \to \mathbb{C}$ is **meromorphic**, if ψ is holomorphic except for poles.*

Example 3. *Rational functions are meromorphic.*

Further, the **Wirtinger derivatives** [GAS17, Ch. 22.2], i.e., linear combinations of the partial derivatives ∂u and ∂v, are introduced as the following partial differential operators

$$\begin{aligned} \frac{\partial}{\partial z} &= \frac{1}{2}\left(\frac{\partial}{\partial u} - i\frac{\partial}{\partial v}\right), \\ \frac{\partial}{\partial \bar{z}} &= \frac{1}{2}\left(\frac{\partial}{\partial u} + i\frac{\partial}{\partial v}\right). \end{aligned}$$

2.3 Complex Projective Geometry

In analog to the real case explained in [Mül20; PW01], homogeneous coordinates are obtained by an embedding in a higher-dimensional space.

Definition 10. *Points in $\mathbb{C}^3$ are associated with points in $\mathbb{C}^4$, namely*

$$\begin{aligned} \hat{} : \mathbb{C}^3 &\to \mathbb{C}^4 \\ z = (z_1, z_2, z_3) &\mapsto (1, z_1, z_2, z_3) =: \hat{z}. \end{aligned}$$

All points on a straight line through the origin differ only by a $\lambda \in \mathbb{C}$ multiple and hence, can be identified via the equivalence relation $x \sim y :\Leftrightarrow \exists \lambda \in \mathbb{C} \setminus \{0\} : x = \lambda y$. The mapping of a point $z \in \mathbb{C}^3$ to its equivalence class $[\hat{z}]$, is called homogenization. Conversely, given a point $\hat{z} = (z_0, z_1, z_2, z_3)$ the rule $\left(\frac{z_1}{z_0}, \frac{z_2}{z_0}, \frac{z_3}{z_0}\right)$ yields again a point in $\mathbb{C}^3$. This procedure is referred to as dehomogenization. Further, the quotient space $\mathbb{C}^{n+1}/\sim =: \mathcal{P}^n$ is called the n-dim complex projective space.

Definition 11. *Let $A \in \mathbb{C}^{(n+1)\times(n+1)} \setminus \{0\}$ be symmetric, i.e., $A = A^\intercal$. Then the set*

$$\{[z] \in \mathcal{P}^n \,|\, z^\intercal A z = 0\} \tag{2.10}$$

is called quadric and in the case of $n = 2$ a conic [PW01, Ch. 1.1.5].

The equation in (2.10) is unique up to a scalar factor $\lambda \neq 0$, since $z^\intercal A z = 0$ implies $z^\intercal \lambda A z = 0$ [Mül20, p. 46].

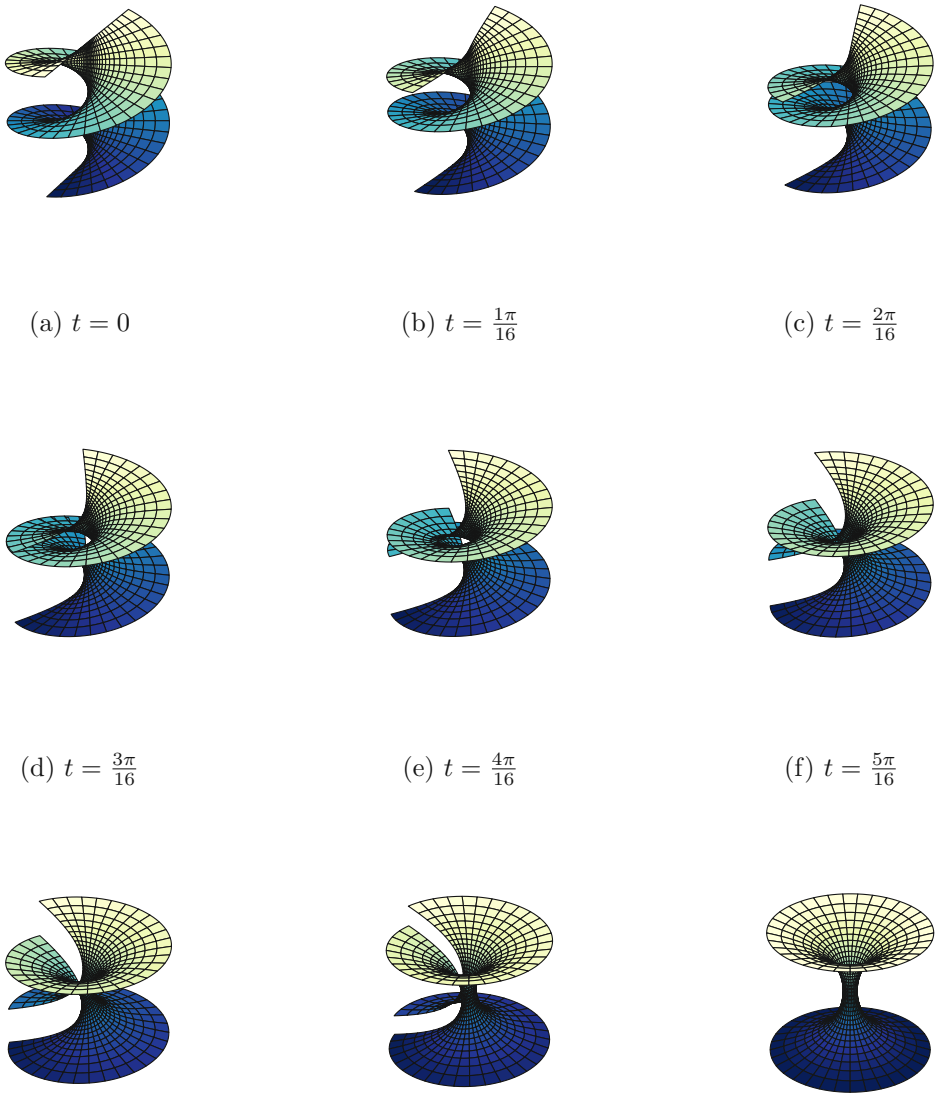

(a) $t = 0$ (b) $t = \frac{1\pi}{16}$ (c) $t = \frac{2\pi}{16}$

(d) $t = \frac{3\pi}{16}$ (e) $t = \frac{4\pi}{16}$ (f) $t = \frac{5\pi}{16}$

(g) $t = \frac{6\pi}{16}$ (h) $t = \frac{7\pi}{16}$ (i) $t = \frac{8\pi}{16}$

Figure 2.2: Deformation helicoid to catenoid.

3 Plateau's Problem

Although the first minimal surfaces, catenoid and helicoid, were known before Plateau, he realized and motivated the connection of minimal surfaces as those with least potential surface energy based on his experiments with soap films. In order to create them, Plateau dipped wires in soapy water. Therefore, the problem named after him is to determine a minimal surface given an arbitrary closed boundary curve.

First existence proofs to Plateau's problem followed approximately 80 years later by Douglas and Radó independently [Dou31; Rad30].

Following [EJ14, Cou37], an existence proof to Plateau's problem is provided for the 3-dimensional case.

Theorem 2 (Plateau's problem)**.** *[EJ14, Ch. 9] Let $\Gamma \subset \mathbb{R}^3$ be a closed $\mathcal{C}^1$-curve without self-intersections. Then there exists a continuous mapping $x : \overline{\mathbb{D}} \to \mathbb{R}^3$, where $\mathbb{D} = \{z \in \mathbb{C} \cong \mathbb{R}^2 : |z| < 1\}$ denotes the unit disk and $\overline{\mathbb{D}}$ it's closure, such that $x|_{\mathbb{D}}$ is a conformal parameterized minimal surface, infinitely differentiable and harmonic on $\mathbb{D}$.*

3.1 Minimal Surface Area

In Section 2.1 minimal surfaces were defined as those surfaces with vanishing mean curvature. This definition, introduced by Lagrange [Lag60], is equivalent to an even more intuitive characterization, namely those of a minimal surface as a critical point of the area functional. The derivation of the latter equivalence is the main part of this section.

Lemma 3. *Let $x : \mathcal{U} \to \mathcal{M}$ be a regular (local) surface. Then for a compact, non-empty set $C \subset \mathcal{U}$ the integral*

$$\int_C \|x_u \times x_v\| \, d(u, v) \tag{3.1}$$

is independent of the chosen patch $x : \mathcal{U} \to \mathcal{M}$ [GAS17, Ch. 12.4,16.1].

Proof. Apply the transformation formula. □

Due to Lemma 3 the following definition of the area of a surface is well-defined [GAS17, Ch. 16.1].

Definition 12. *Under the assumption of Lemma 3 the area $x(C)$ is defined as*

$$\mathcal{A}(x(C)) := \int_C \|x_u \times x_v\| \, d(u, v). \tag{3.2}$$

It can be further calculated, that $\|x_u \times x_v\| = \sqrt{EG - F^2}$, where E, F and G are the coefficients of the first fundamental form. Next, the relationship of a minimal surface, as a surface of vanishing mean curvature and the surface of least area among the family of surfaces with a given closed boundary curve will be explained.

Definition 13. *Let $x : \mathcal{U} \to \mathbb{R}^3$ be a regular local surface, $\mathcal{S} \subset \mathcal{U}$ be a bounded region in $\mathcal{U}$ and let $N(u, v)$ denote the unit vector field normal to $x(u, v)$ for any $(u, v) \in \mathcal{U}$. The* ***normal variation*** *[GAS17, Ch. 16.1] of x under any differentiable mapping $h : \mathcal{S} \to \mathbb{R}$ and $\epsilon > 0$ is defined as*

$$X : (-\epsilon, \epsilon) \times \mathcal{S} \longrightarrow \mathbb{R}^3 \tag{3.3}$$

$$(t, (u, v)) \longmapsto x(u, v) + th(u, v)N(u, v). \tag{3.4}$$

In the following we use the abbreviation $X^t(u, v) := X(t, (u, v))$.

The normal variation X^t describes for each t a slightly deformed (local) surface in normal direction and hence, to indicate the t different first fundamental forms, we use the notation

$$E^t = \langle X^t_u, X^t_u \rangle, F^t = \langle X^t_u, X^t_v \rangle \text{ and } G^t = \langle X^t_v, X^t_v \rangle. \tag{3.5}$$

In preparation for the main result in this section, the relation of a vanishing mean curvature to a minimal surface area, the so-called first variation of a surface will be derived [GAS17, Ch. 16.1].

Lemma 4. *Let $\mathcal{A}(t) = \int_{\mathcal{S}} \|X^t_u \times X^t_v\| \, d(u, v)$ denote the area of each normal variation $X^t(\mathcal{S})$. Then the first variation of $\mathcal{A}$, i.e., $\left(\frac{d\mathcal{A}}{dt}\right)\big|_{t=0}$, is*

$$\left(\frac{d\mathcal{A}}{dt}\right)\Big|_{t=0} = -2 \int_{\mathcal{S}} hH\sqrt{EG - F^2} \, d(u, v), \tag{3.6}$$

where H is the mean curvature of $\mathcal{S}$.

Proof. First, note that by the remark below of Definition 12 and Equation (3.5)

$$\mathcal{A}(t)(X^t(S)) = \int_{\mathcal{S}} \|X^t_u \times X^t_v\| \, d(u, v) = \int_{\mathcal{S}} \sqrt{E^t G^t - (F^t)^2} \, d(u, v).$$

Starting with E^t, G^t and F^t will be subsequently calculated.

$$\begin{aligned}
E^t &= \langle X^t_u, X^t_u \rangle \\
&= \langle x_u + th_u N + thN_u, x_u + th_u N + thN_u \rangle \\
&= \langle x_u, x_u \rangle + \langle x_u, th_u N \rangle + \langle x_u, thN_u \rangle + \langle th_u N, x_u \rangle + \langle thN_u, x_u \rangle + \mathcal{O}(t^2) \\
&= E + 2\langle x_u, th_u N \rangle + 2\langle x_u, thN_u \rangle + \mathcal{O}(t^2) \\
&= E + 2th_u \underbrace{\langle x_u, N \rangle}_{=0} - 2th\langle N, x_{uu} \rangle + \mathcal{O}(t^2) \\
&= E - 2the + \mathcal{O}(t^2).
\end{aligned}$$

Analogously,

$$\begin{aligned} F^t &= F - 2thf + \mathcal{O}(t^2) \text{ and} \\ G^t &= G - 2thg + \mathcal{O}(t^2), \end{aligned}$$

where e, f and g are the coefficients of the second fundamental form. Furthermore, using Lemma 2 it can be derived that

$$\begin{aligned} E^tG^t - (F^t)^2 &= \left(E - 2the + \mathcal{O}(t^2)\right)\left(G - 2thg + \mathcal{O}(t^2)\right) - \left(F - 2thf + \mathcal{O}(t^2)\right)^2 \\ &= EG - F^2 - 2thgE - 2theG + 4thfF + \mathcal{O}(t^2) \\ &= EG - F^2 - 2th(eG - 2fF + gE) + \mathcal{O}(t^2) \\ &= EG - F^2 - 4thH(EG - F^2) + \mathcal{O}(t^2) \\ &= (EG - F^2)(1 - 4thH) + \mathcal{O}(t^2) \end{aligned}$$

and hence,

$$\begin{aligned} \sqrt{E^tG^t - (F^t)^2} &= \sqrt{(EG - F^2)(1 - 4thH) + \mathcal{O}(t^2)} \\ &= \sqrt{(EG - F^2)}\sqrt{(1 - 4thH) + \mathcal{O}(t^2)} \\ &= \sqrt{(EG - F^2)}\sqrt{(1 - 2thH)^2 + \mathcal{O}(t^2)} \\ &= \sqrt{(EG - F^2)}(1 - 2thH) + \mathcal{O}(t^2). \end{aligned}$$

In conclusion, the first variation is given as

$$\begin{aligned} \left(\frac{d\mathcal{A}}{dt}\right)\Big|_{t=0} &= \left(\frac{d}{dt}\int_{\mathcal{S}} \sqrt{(EG - F^2)}(1 - 2thH) + \mathcal{O}(t^2)\, d(u,v)\right)\Big|_{t=0} \\ &= -2\int_{\mathcal{S}} hH\sqrt{(EG - F^2)}. \end{aligned}$$

□

Theorem 3. *Let $x : \mathcal{U} \to \mathbb{R}$ be a regular surface and $\mathcal{S} \subset \mathcal{U}$. Then x is a critical point of the area functional on $\mathcal{S}$ if and only if the mean curvature H vanishes [GAS17, Ch. 16.1].*

Proof. First, let the mean curvature be identically zero, i.e., $H = 0$, then by (3.6) in Lemma 4 the first variation is zero for each h and therefore, $X^0 = x$ is a critical point of the area functional.

For the other direction, assume the contrary, i.e., $\left(\frac{d\mathcal{A}}{dt}\right)\Big|_{t=0} = 0$ for any differentiable $h : \mathcal{S} \to \mathbb{R}$ and there is a point $p := (\bar{u}, \bar{v}) \in \mathcal{S}$ such that the mean curvature $H(p) \neq 0$. Since h is arbitrary and smooth, choose h such that $h(p) = H(p)$ in a small neighborhood $B_\epsilon(p)$ around p and zero outside. Again by (3.6) and the positive definiteness of the first fundamental form,

$$\left(\frac{d\mathcal{A}}{dt}\right)\Big|_{t=0} = -2\int_{\mathcal{S}} \underbrace{H^2\sqrt{EG - F^2}}_{\geq 0}\, d(u,v) < 0,$$

which contradicts the assumption that the first variation equals zero. Hence, the mean curvature $H(p) = 0$ for any arbitrary p. □

Since, x is only a critical point it is uncertain whether the obtained surface is actually minimal. There are cases, where x is not necessary a minimum, which is discussed in detail in [She22; Nit89].

3.2 Harmonic Functions

Some major properties of harmonic functions, i.e., functions h such that $\Delta h = 0$, which result from Poisson's representation are repeated in this section, for details see [EJ14, Ch. 9.7].

Theorem 4 (Mean value property of harmonic functions)**.** *Let $h : B_R(0) \to \mathbb{R}$ be harmonic and let $\rho < R$, then the mean value property holds*

$$h(0) = \frac{1}{\alpha_n \rho^{n-1}} \int_{\partial B_\rho(0)} h, \tag{3.7}$$

where α_n is the surface area of the unit sphere.

Corollary 1. *Let h be as in Theorem 4, then integration over ρ from 0 to $r < R$ implies*

$$h(0) = \frac{1}{\mathrm{vol}(B_r(0))} \int_{B_r} h. \tag{3.8}$$

Theorem 5 (Maximum principle)**.** *A harmonic, non-constant function h on $\mathbb{D}$ has no minimum or maximum on $\mathbb{D}$.*

Proof. Assume h has a maximum at $x_0 \in \mathbb{D}$. For proving that there is no minimum consider $-h$. First, define a function that is harmonic and has it's maximum at $x = 0$,

$$f(x) := h(x - x_0) - h(x_0).$$

Then for small $r > 0$,

$$0 = f(0) \geq f(x) \ \forall x \in B_r(0). \tag{3.9}$$

Next, we show equality for (3.9). Assume $f \leq 0$ on $B_r(0)$ and at some point even $f < 0$. Since, f is smooth the function $f < 0$ in an open subset of $B_r(0)$. But then by the mean value property of harmonic functions, Theorem 4, and it's corollary

$$0 = f(0) = \frac{1}{\mathrm{vol}(B_r(0))} \int_{B_r(0)} < 0,$$

leads to a contradiction. Hence,

$$0 = f(0) = f(x) = h(x - x_0) - h(x_0) \ \forall x \in B_r(0)$$

and $h(x) = h(x_0)$ for all $x \in B_r(0)$. Since, the set $\{x \in \mathbb{D} : h(x) = h(x_0)\}$ is open, relative closed and connected in $\mathbb{D}$, h is constant $h(x_0)$, which contradicts the assumption of a non-constant h. □

3.3 Dirichlet Integral and Dirichlet's Principle

The so-called Dirichlet energy is closely related to the area functional of a smooth, conformal mapping, cf. Lemma 5 [EJ14, Ch.9.3]. Using this relationship it suffices to minimize the Dirichlet integral given a concrete continuous boundary curve γ. As in [EJ14, Ch. 9.3,Ch. 9.7] we first show Dirichlet's principle for a smooth boundary, Theorem 7, and then using the maximum principle for harmonic functions, Theorem 5, as well as Harnack's principle, Theorem 6, we extend the Dirichlet principle to continuous boundary values, Theorem 8.

Definition 14. *A function $x : \mathcal{U} \to \mathbb{R}^n$ is called **weak conformal** if $||x_u|| = ||x_v||$ and $\langle x_u, x_v\rangle = 0$, where x_u may contain zeros.*

Definition 15. *Let*

$$\mathcal{D}(x) = \frac{1}{2}\int_{\mathbb{D}} (g_{uu} + g_{vv}), \tag{3.10}$$

*where $g_{ij} = \langle x_i, x_j\rangle$ and x_i is the partial derivative with respect to the i-th component, denote the **Dirichlet integral**.*

Lemma 5. *Let $x \in C^1(\mathbb{D}, \mathbb{R}^n)$ be weak conformal, then $\mathcal{A}(x)$ is minimal if and only if $\mathcal{D}(x)$ is minimal.*

Proof. Since, $||x_u|| = ||x_v||$ implies $g_{uu} = \langle x_u, x_u\rangle = \langle x_v, x_v\rangle = g_{vv}$ and $g_{uv} = \langle x_u, x_v\rangle = 0$, we have

$$\mathcal{D}(x) = \frac{1}{2}\int_{\mathbb{D}} (g_{uu} + g_{vv}) = \int_{\mathbb{D}} g_{uu} = \int_{\mathbb{D}} \sqrt{(g_{uu})^2} = \int_{\mathbb{D}} \sqrt{g_{uu}g_{vv}} = \int_{\mathbb{D}} \sqrt{g_{uu}g_{vv} - g_{uv}^2} = \mathcal{A}(x).$$

□

Theorem 6 (Harnack's principle)**.** *Let $(h_k)_{k\in\mathbb{N}}$ be a sequence of continuous functions on $\overline{\mathbb{D}}$ that are harmonic on $\mathbb{D}$ and uniformly convergent on $\partial\mathbb{D}$, then all (h_k) and their partial derivatives converge uniformly on $\mathbb{D}$ to a harmonic function h_∞. Moreover, the following estimate for the Dirichtlet integral of the limit h_∞ holds*

$$\mathcal{D}(h_\infty) \leq \liminf_{k\to\infty} \mathcal{D}(h_k).$$

Proof. A proof is provided in [EJ14, Ch. 9.7] □

Theorem 7 (Dirichlet's principle for smooth boundaries)**.** *Let $\gamma \in C^1(\partial\mathbb{D}, \mathbb{R}^n)$ and $h \in C^1(\overline{\mathbb{D}}, \mathbb{R}^n) \cap C^2(\mathbb{D}, \mathbb{R}^n)$ be harmonic on $\mathbb{D}$, i.e., $\Delta\, h|_{\mathbb{D}} = 0$ and values γ on $\partial\mathbb{D}$, i.e., $h|_{\partial\mathbb{D}} = \gamma$, then*

$$\mathcal{D}(h) \leq \mathcal{D}(f), \tag{3.11}$$

for all $f \in C^1(\overline{\mathbb{D}}, \mathbb{R}^n)$ with $f|_{\partial\mathbb{D}} = \gamma$.

Proof. By Equation 15 for $h = (h^1, \dots, h^j, \dots, h^n)$, where h^j is the j-th component of the vector valued function h the following identity can be derived

$$\mathcal{D}(h) = \frac{1}{2}\int_{\mathbb{D}} |\partial h|^2 = \frac{1}{2}\int_{\mathbb{D}} \sum_j |\partial h^j|^2 = \frac{1}{2}\sum_j \int_{\mathbb{D}} |\partial h^j|^2 = \sum_j \mathcal{D}(h^j).$$

Minimizing every component $\mathcal{D}(h^j)$, $j = 1, \dots, n$, is therefore equivalent in order to minimize $\mathcal{D}(h)$ and w.l.o.g. we can assume $n = 1$. Defining $k := f - h$, it follows

$$\mathcal{D}(f) = \frac{1}{2}\int_{\mathbb{D}} |\partial f|^2 = \frac{1}{2}\int_{\mathbb{D}} |\nabla f|^2 = \frac{1}{2}\int_{\mathbb{D}} \left(|\nabla h|^2 + |\nabla k|^2 + 2\langle \nabla h, \nabla k\rangle\right). \tag{3.12}$$

Further, since h is harmonic, i.e., $\Delta h = 0$

$$\langle \nabla h, \nabla k\rangle = \langle \nabla h, \nabla k\rangle + k \cdot \Delta h = \langle \nabla h, \nabla k\rangle + k \cdot \operatorname{div}(\nabla h) = \operatorname{div}(k \cdot \nabla h). \tag{3.13}$$

Continuing (3.12) and using (3.13) as well as Gaussian divergence theorem, Theorem 19, the following holds

$$\frac{1}{2}\int_{\mathbb{D}} |\nabla h|^2 + |\nabla k|^2 + \int_{\mathbb{D}} \operatorname{div}(k \cdot \nabla h) = \mathcal{D}(h) + \mathcal{D}(k) + \int_{\partial\mathbb{D}} \langle k \cdot \nabla h, \nu\rangle, \tag{3.14}$$

where ν is the outer normal on the boundary $\partial\mathbb{D}$. The rightmost term in (3.14) vanishes as $k = 0$ on $\partial\mathbb{D}$ and we conclude

$$\mathcal{D}(f) = \mathcal{D}(h) + \mathcal{D}(k) \geq \mathcal{D}(h).$$

□

Theorem 8 (Dirichlet's principle for continuous boundaries)**.** *Let $\gamma \in C^0(\partial\mathbb{D}, \mathbb{R}^n)$ and $h \in C^0(\overline{\mathbb{D}}, \mathbb{R}^n) \cap C^2(\mathbb{D}, \mathbb{R}^n)$ be harmonic on $\mathbb{D}$, i.e., $\Delta\, h|_{\mathbb{D}} = 0$ and values γ on $\partial\mathbb{D}$, i.e., $h|_{\partial\mathbb{D}} = \gamma$, then*

$$\mathcal{D}(h) \leq \mathcal{D}(f) \tag{3.15}$$

for all $f \in C^0(\overline{\mathbb{D}}, \mathbb{R}^n) \cap C^1(\mathbb{D}, \mathbb{R}^n)$ with $f|_{\partial\mathbb{D}} = \gamma$.

Proof. Assume the contrary, $f \in C^0(\overline{\mathbb{D}}) \cap C^1(\mathbb{D})$ with $f|_{\partial\mathbb{D}} = \gamma$ and

$$\mathcal{D}(f) < \mathcal{D}(h).$$

First, define the set

$$D_k := \{z \in \mathbb{C} : |z| < 1 - \frac{1}{k}\},$$

which is a subset of $\mathbb{D}$ and let $h_k|_{\partial D_k} = f|_{\partial D_k}$. By assumption $f \in C^0(\overline{\mathbb{D}}) \cap C^1(\mathbb{D})$ and hence, the restriction , $f|_{\partial D_k}$, to $D_k \subset \mathbb{D}$ is a C^1-mapping. Similar, $h \in C^2(D_k)$ and $\Delta h = 0$

on $\mathbb{D}$ implies $\Delta\, h_k|_{D_k} = 0$. By Dirichlet's principle for smooth boundaries, Theorem 7, the following holds for the energy

$$\mathcal{D}(h_k) \leq \mathcal{D}(g)$$

for all $g \in C^1(\overline{D}_k)$ with $g|_{\partial D_k} = f|_{\partial D_k}$. In particular, the above energy estimate applies to $f|_{D_k}$ and we define

$$f_k := \begin{cases} f, \text{ on } \overline{\mathbb{D}} \setminus D_k \\ h_k, \text{ on } D_k. \end{cases}$$

By definition, f_k has the following property

$$\begin{aligned} \mathcal{D}(f_k) &= \mathcal{D}(\,f_k|_{\mathbb{D}\setminus D_k}) + \mathcal{D}(\,f_k|_{D_k}) \\ &= \mathcal{D}(\,f|_{\mathbb{D}\setminus D_k}) + \mathcal{D}(h_k) \\ &\leq \mathcal{D}(\,f|_{\mathbb{D}\setminus D_k}) + \mathcal{D}(\,f|_{D_k}) = \mathcal{D}(f). \end{aligned}$$

Next, consider

$$\tilde{h}_k(u) = h_k(\frac{k-1}{k}u)$$

for $u \in \overline{\mathbb{D}}$, which are, contrary to f_k, harmonic on $\mathbb{D}$. Since, f is continuous, the boundary values $\tilde{h}_k(t) = f(\frac{k-1}{k}t)$ for $t \in \partial\mathbb{D}$ converge uniformly and Harnack's principle, Theorem 6 implies the local convergence of $\tilde{h}_k$ and all their partial derivatives on $\mathbb{D}$ to a function h_∞ with the property that

$$\mathcal{D}(h_\infty) \leq \liminf_{k\to\infty} \mathcal{D}(\tilde{h}_k).$$

And further, by the initial assumption

$$\mathcal{D}(h) > \mathcal{D}(f) > \mathcal{D}(\tilde{h}_k) \geq \liminf_{k\to\infty} \geq \mathcal{D}(h_\infty).$$

So, $h_\infty \neq h$, h_∞ is harmonic on $\mathbb{D}$ and $h_\infty|_{\partial\mathbb{D}} = \gamma$. But then the difference $h_\infty - h$ is harmonic on $\mathbb{D}$ with $(h_\infty - h)|_{\partial\mathbb{D}} = 0$ and $(h_\infty - h)$ would have a minimum or maximum value on $\mathbb{D}$, which is a contradiction to the maximum principle, Theorem 5. □

3.4 Independence of the concrete Parametrization

So far, the specific parametrization γ was specified. Now in this section, based on [EJ14, Ch. 9.4], the Dirichlet integral is minimized over all possible parametrization of $\Gamma = \gamma(\partial\mathbb{D})$. Therefore, a parametrization $\gamma : \partial\mathbb{D} \to \Gamma$ with the property that the corresponding harmonic function h_γ, where h_γ denotes a function such that the restriction to $\partial\mathbb{D}$ equals γ, on $\mathbb{D}$ has minimal energy, i.e.,

$$\mathcal{D}(h_\gamma) \leq \mathcal{D}(h_{\tilde{\gamma}})$$

for all parametrization $\tilde{\gamma} : \partial\mathbb{D} \to \Gamma$.

First, define the set of functions, mapping the boundary $\partial\mathbb{D}$ monotone to Γ,

$$F_\Gamma = \{f \in C^1(\mathbb{D}) \cap C^0(\overline{\mathbb{D}}) : f(\partial\mathbb{D}) = \Gamma,\ f|_{\partial D} : \partial\mathbb{D} \nearrow \Gamma\} \tag{3.16}$$

and

$$d(\Gamma) := \inf\{\mathcal{D}(f) : f \in F_\Gamma\}. \tag{3.17}$$

Choose a sequence (f_k) in F_Γ such that $\mathcal{D}(f_k) \longrightarrow d(\Gamma)$. Then by Dirichlet's principle for a continuous boundary, Theorem 8, the harmonic functions with same boundary values minimize the Dirichlet integral. Hence, consider a harmonic sequence (h_k) with $h_k|_{\partial\mathbb{D}} = f_k|_{\partial\mathbb{D}}$. If the conditions for Harnack's principle, Theorem 6, hold, then for the on $\mathbb{D}$ harmonic limit $h = \lim h_k$

$$d(\Gamma) \leq \mathcal{D}(h) \leq \liminf_{k\to\infty} h_k \leq \liminf_{k\to\infty} f_k = d(\Gamma),$$

holds and implies $\mathcal{D}(h) = d(\Gamma)$ as long as $\mathcal{D}(f) > E$ for some E with $E > d(\Gamma)$. In order to apply Harnack's principle, a uniformly convergence of the boundary values $\gamma_k = f_k|_{\partial D}$ is necessary. However, since $\mathcal{D}$ is invariant under conformal parameter changes, Lemma 6, an energy minimizing sequence f_k with $f_k(\partial D) = \Gamma$ and uniformly convergent on ∂D can be modified by a conformal parameter change ϕ such that $\tilde{f}_k := f_k \circ \phi$ is still energy minimizing, but has no convergent subsequence, see Example 4.

Lemma 6. *The Dirichlet integral $\mathcal{D}$ is invariant under conformal parameter changes $\phi : \overline{\mathbb{D}} \to \overline{\mathbb{D}}$, i.e.,*

$$\mathcal{D}(x \circ \phi) = \mathcal{D}(x).$$

Proof. Since, ϕ is conformal it's derivative has the form $\partial\phi = \begin{pmatrix} a & -b \\ b & a \end{pmatrix}$ and so, $\det(\partial\phi) = \left(a^2 + b^2\right)$. Further,

$$\begin{aligned} \partial(x \circ \phi) &= \partial x_\phi \partial\phi = (x_u, x_v) \begin{pmatrix} a & -b \\ b & a \end{pmatrix} \\ &= (ax_u + bx_v, -bx_u + ax_v) \end{aligned}$$

and hence,

$$\begin{aligned} |\partial(x \circ \phi)|^2 &= |ax_u + bx_v|^2 + |-bx_u + ax_v|^2 \\ &= (a^2 + b^2)(|x_u|^2 + |x_v|^2) \\ &= |\det(\partial\phi)||\partial X_\phi|. \end{aligned}$$

Due to transformation theorem, it can be concluded

$$\mathcal{D}(x \circ \phi) = \int_{\mathbb{D}} |\partial(x \circ \phi)|^2 = \int_{\mathbb{D}} |\partial x_\phi|^2 |\det(\partial\phi)| = \int_{\mathbb{D}} |\partial x|^2 = \mathcal{D}(x).$$

□

Example 4. *Let $f_k : \mathbb{D} \to \mathbb{R}$ be an energy minimizing sequence of functions, i.e., $\mathcal{D}(f_k) \longrightarrow d(\Gamma)$, with $f_k(\partial D) = \Gamma$ and uniformly convergent on $\partial\mathbb{D}$. There is a conformal parameter change ϕ_k such that $\tilde{f}_k := f_k \circ \phi_k$ is still energy minimizing, but it has no convergent subsequence.*

Due to Example 4, just certain parameter changes can be considered and hence, instead of (3.16) the more restrictive set

$$\tilde{F}_\Gamma = \{f \in F_\Gamma : f(z_i) = p_i, i = 1, 2, 3 \text{ with } p_i \in \Gamma \text{ and } \mathcal{D}(f) \leq E\} \tag{3.18}$$

will be of further interest, where p_i, for $i = 1, 2, 3$, are three arbitrary values. This set is well-defined, because for any triple $x_1 < x_2 < x_3$ and $y_1 < y_2 < y_3$ there is a unique linear, rational mapping f such that $f(x_i) = y_i$, $i = 1, 2, 3$.

Using the Lemma of Courant and Lebesgue, Lemma 7, as well as Arzelà-Ascoli, Theorem 20, it can be verified that every sequence in $\tilde{F}_\Gamma$ has a uniformly convergent subsequence.

Lemma 7 (Courant-Lebesgue)**.** *Let $z_0 \in \partial\mathbb{D}$ and $k_r = \partial B_r(z_0) \cap \overline{\mathbb{D}}$, $r > 0$, the arc in $\overline{\mathbb{D}}$ with center z_0. Then for every $\epsilon > 0$ there is $\delta \in (0, 1)$ such that for arbitrary $f \in \tilde{F}_\Gamma$ there is $\bar{r} \in (\delta, \sqrt{\delta})$ and the length of curve $k_{\bar{r}}$ under f can be estimated as*

$$\mathcal{L} := \int |(f \circ k_{\bar{r}})'| < \epsilon. \tag{3.19}$$

Proof. See [EJ14, Ch. 9.4]. □

Lemma 8. *Let $f \in \tilde{F}_\Gamma\Big|_{\partial\mathbb{D}} := \{f|_{\partial\mathbb{D}} : f \in \tilde{F}_\Gamma\}$. Then the image of the partial curve $\partial\mathbb{D}_{z_s z_e} := \partial\mathbb{D} \cap \bar{B}_{\bar{r}}(z_0) \subset \partial\mathbb{D}$ with endpoints denoted as z_s, z_e and $z_0 \in \partial\mathbb{D}$, under f is a subset of $B_\epsilon(f(z_s))$, i.e., $f(\partial\mathbb{D}_{z_s z_e}) \subset B_\epsilon(f(z_s))$.*

Proof. Using the additional condition in (3.18) and $\partial\mathbb{D}$ is monotone mapped to Γ. □

Lemma 9. *The set $\tilde{F}_\Gamma \restriction_{\partial D}$ is equicontinuous.*

Proof. Consider an arbitrary point $z_0 \in \partial\mathbb{D}$ and the arc $k_{\bar{r}} = \partial B_{\bar{r}}(z_0)$, which divides the boundary of $\partial\mathbb{D}$ into two parts, $\partial\mathbb{D}_{z_s z_e} := \partial\mathbb{D} \cap \bar{B}_{\bar{r}}(z_0)$ and it's complement $\big(\partial\mathbb{D} \cap \bar{B}_{\bar{r}}(z_0)\big)^c$. As in the above lemma let z_s and z_e denote the endpoints of $\partial\mathbb{D}_{z_s z_e}$. Since, $\Gamma = \gamma(\partial\mathbb{D})$ is a vector-valued, closed $\mathcal{C}^1$-curve, let $\epsilon > 0$ be so small such that the tangent at $p := f(z_s)$ is a "good" approximation of the arc $\Gamma \cap B_\epsilon(p)$.

Due to Courant-Lebesgue, Lemma 7, for ϵ there is $\delta \in (0, 1)$ such that for any arbitrary $f \in \tilde{F}_\Gamma$ there is $\bar{r} \in (\delta, \sqrt{\delta})$ with $\mathcal{L}(f \circ k_{\bar{r}}) < \epsilon$ and hence, the difference of $f(z_s)$ and $f(z_e)$ can be estimated as

$$|f(z_s) - f(z_e)| \leq |\mathcal{L}(f \circ k_{\bar{r}})| < \epsilon.$$

Now, by the above Lemma 8, the image $f(\partial\mathbb{D} \cap \bar{B}_{\bar{r}}(z_0))$ is contained in $B_\epsilon(f(z_s))$ and it can be concluded

$$|f(z) - f(z_0)| < 2\epsilon$$

for all $z \in \partial\mathbb{D}$ with $|z - z_0| < \delta < \bar{r}$, which shows the equicontinuity. □

In conclusion, there are solutions to Plateau's problem:

Theorem 9. *There exists an energy minimizing and on $\mathbb{D}$ harmonic function $h \in \tilde{F}_\Gamma$.*

Proof. The solution is constructed as the limit h of a sequence (h_k) of harmonic functions. First, the inequality $\mathcal{D}(h) \leq d(\Gamma)$ will be proved. Consider therefore, a sequence $(f_k) \in \tilde{F}_\Gamma$ with $\mathcal{D}(f_k) \longrightarrow d(\Gamma)$ and replace it with on $\mathbb{D}$ harmonic functions (h_k) and $h_k|_{\partial\mathbb{D}} = f_k|_{\partial\mathbb{D}}$. Then $(h_k) \in \tilde{F}_\Gamma$ and the restriction to $\partial\mathbb{D}$ is by Lemma 9 equicontinuous and pointwise bounded. Using the Theorem of Arzelà-Ascoli, Theorem 20, there exists a uniformly convergent subsequence (h_{k_j}) on $\partial\mathbb{D}$. Further, Harnack's principle, Theorem 6, implies that this subsequence (h_{k_j}) converges uniformly on $\mathbb{D}$ to a harmonic function h and

$$\mathcal{D}(h) \leq \liminf_{j\to\infty}(h_{k_j}) = d(\Gamma).$$

Next, if $h \in \tilde{F}_\Gamma$ then the other inequality $\mathcal{D}(h) \geq d(\Gamma)$ would follow. Since, (h_{k_j}) converges uniformly to h and all (h_{k_j}) satisfy the condition that $h(z_i) = p_i$, so does h. Analogously, $h|_{\partial\mathbb{D}} : \partial\mathbb{D} \to \Gamma$ is monotone and surjective. It can be concluded that $h \in \tilde{F}_\Gamma$ and $\mathcal{D}(h) = d(\Gamma)$ with $\Delta h|_{\mathbb{D}} = 0$. □

That the so constructed solution of Theorem 2 is weak conformal, follows, inter alia, from Lemma 5. Assume $x : \mathbb{D} \to \mathbb{R}^3$ would not be weak conformal, then, using the existence of conformal parameters [Küh15], there is a parameter transformation $\phi : \mathbb{D} \to \mathbb{D}$ such that $\tilde{x} = x \circ \phi$ is weak conformal and by Lemma 5, $\mathcal{D}(\tilde{x}) = \mathcal{A}(\tilde{x})$. Moreover, by the invariance of the area under parameter changes, Lemma 3, $\mathcal{A}(\tilde{x}) = \mathcal{A}(x)$, and the inequality of arithmetic and geometric means, $\mathcal{A}(x) < \mathcal{D}(x)$, yields the contradiction $\mathcal{D}(\tilde{x}) < \mathcal{D}(x)$. We do not explicitly exclude isolated branching points, i.e., zeros of the derivative of x, like [Dou31; Rad30], since we only approach the problem in 3-dimensions and Osserman proved that in this case there are no branching points, for details see [Oss70] .

4 Weierstrass Representation

An essential scientific achievement regarding the generation of minimal surfaces can be traced back to Weierstrass in 1866. He showed a one-to-one relationship of isotropic, holomorphic functions to minimal surfaces. Thus, using the famous Weierstrass representation formula, one can easily construct minimal surfaces [GAS17, Ch. 22; EJ14, Ch. 8].

4.1 Isotropic Differential Geometry

Definition 16. *A complex-valued vector $v \in \mathbb{C} \setminus \{0\}$ is **isotropic**, if*

$$\langle v, v \rangle = 0 \tag{4.1}$$

holds.

Definition 17. *Let $\mathcal{U}$ be an open subset of $\mathbb{C}$. A holomorphic function $\psi : \mathcal{U} \to \mathbb{C}^n$ such that the complex derivative $\psi'(z)$ is isotropic for all $z \in \mathcal{U}$, i.e.,*

$$\langle \psi'(z), \psi'(z) \rangle = 0, \text{ for all } z \in \mathcal{U} \tag{4.2}$$

*is called a **minimal curve**.*

One of the first known minimal surfaces obtained using complex analysis was found by Enneper [Enn68].

Example 5. *The following holomorphic function*

$$Enn_n : \begin{cases} \mathbb{C} \to \mathbb{C}^3 \\ z \mapsto \left(z - \frac{z^{2n+1}}{2n+1}, iz + \frac{iz^{2n+1}}{2n+1}, \frac{2z^{n+1}}{n+1} \right), \end{cases}$$

*satisfies Equation (4.2). This minimal curve is denoted as **Enneper's minimal surface of degree** n, cf. Figure 4.1.*

The next result displays how the mean curvature is related to the Laplacian of a conformal parametrization [EJ14, Ch. 8.4; GAS17, Ch.16.7].

Lemma 10. *The mean curvature H of a conformal parametrization $\psi : \mathcal{U} \to \mathbb{R}^3$ satisfies*

$$\Delta \psi = 2\lambda^2 H N,$$

where λ is a scaling factor and N denotes the Gaussian unit normal.

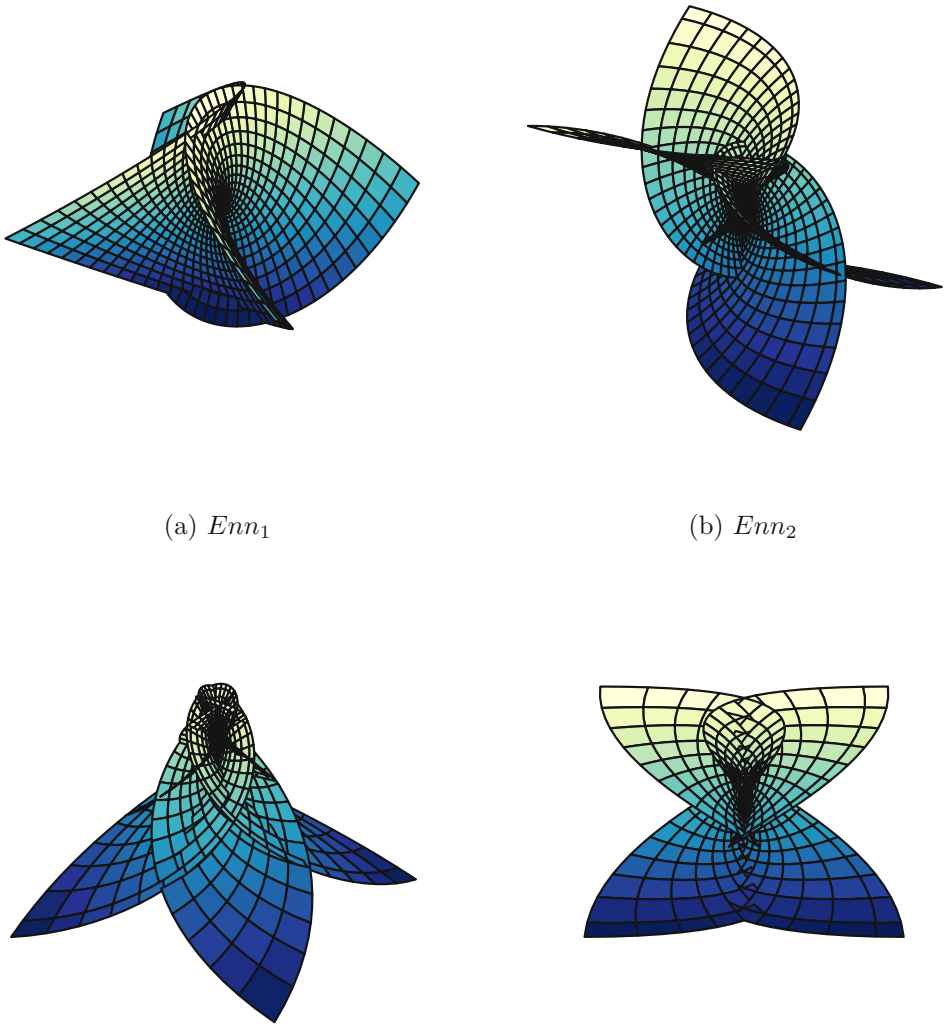

(a) Enn_1 (b) Enn_2

(c) Enn_3 (d) Enn_4

Figure 4.1: Enneper's surfaces of degree 1 to 4.

Proof. First, we show that $\Delta\psi$ is normal to the tangential space at (u, v), spanned by (ψ_u, ψ_v). The Equations (2.5) are therefore differentiated with respect to u and v, respectively.

$$\begin{aligned} \langle \psi_{uv}, \psi_v \rangle &= \langle \psi_{uu}, \psi_u \rangle \\ \langle \psi_{uv}, \psi_v \rangle &= -\langle \psi_u, \psi_{vv} \rangle \end{aligned}$$

Subtracting the first from second equation and basic calculations yield

$$\begin{aligned} 0 &= \langle \psi_{uu}, \psi_u \rangle + \langle \psi_{vv}, \psi_u \rangle \\ &= \langle \psi_{uu} + \psi_{vv}, \psi_u \rangle \\ &= \langle \Delta\psi, \psi_u \rangle . \end{aligned}$$

Analogously, $\langle \Delta\psi, \psi_v \rangle = 0$ is verified. Since, $\Delta\psi$ is normal to the tangential space at (u, v) it has to be a multiple of the Gaussian unit normal N. Using Lemma 2 resp. formula (2.6) in the following remark and the assumption that ψ is conformally parameterized, i.e., $F = \langle \psi_u, \psi_v \rangle = 0$ and $||x_u|| = ||x_v|| =: \lambda$, we calculate

$$H = \frac{e+g}{2E} = \frac{e+g}{2\lambda^2} = \frac{\langle \psi_{uu} + \psi_{vv}, N \rangle}{2\lambda^2},$$

and conclude

$$\Delta\psi = 2\lambda^2 H N.$$

□

In particular, Lemma 10 implies that harmonic functions are conformally parameterized minimal surfaces [GAS17, Ch. 22.1], which is summarized in the following corollary.

Corollary 2. *A conformal parametrization $\psi : \mathcal{U} \to \mathbb{R}^3$ is a minimal surface if and only if it is harmonic.*

Theorem 10. *$\psi : \mathcal{U} \to \mathbb{R}^n$ is a conformally parameterized minimal surface if and only if $\psi_z : \mathcal{U} \to \mathbb{C}^n$ is isotropic.*

Proof. Due to the following identity

$$\begin{aligned} \langle \psi_z, \psi_z \rangle &= \frac{1}{4} \left\langle \left(\frac{\partial \psi_1}{\partial u} - i\frac{\partial \psi_1}{\partial v}, ..., \frac{\partial \psi_n}{\partial u} - i\frac{\partial \psi_n}{\partial v} \right), \left(\frac{\partial \psi_1}{\partial u} - i\frac{\partial \psi_1}{\partial v}, ..., \frac{\partial \psi_n}{\partial u} - i\frac{\partial \psi_n}{\partial v} \right) \right\rangle \\ &= \frac{1}{4} \sum_{j=1}^{n} \left(\frac{\partial \psi_j}{\partial u} - i\frac{\partial \psi_j}{\partial v} \right)^2 \\ &= \frac{1}{4} \sum_{j=1}^{n} \left(\frac{\partial \psi_j}{\partial u}^2 - 2i\frac{\partial \psi_j}{\partial u}\frac{\partial \psi_j}{\partial v} - \frac{\partial \psi_j}{\partial v}^2 \right) \\ &= \frac{1}{4} \left(\langle \psi_u, \psi_u \rangle - 2i \langle \psi_u, \psi_v \rangle - \langle \psi_v, \psi_v \rangle \right) \\ &= \frac{1}{4} \left(||\psi_u||^2 - 2i \langle \psi_u, \psi_v \rangle - ||\psi_v||^2 \right) \end{aligned}$$

ψ is a conformal parametrization if and only if ψ_z is isotropic. Since, ψ is holomorphic and satisfies $0 = \psi_{z\bar{z}} = \psi_{\bar{z}z} = \frac{1}{4}\Delta\psi$, ψ is a minimal surface due to Corollary 2. □

Theorem 10 can be used to verify Enneper's surfaces, cf. Example 5, as minimal surfaces.

Example 6. *The Enneper's surfaces of degree n, defined in Example 5, are minimal surfaces.*

$$\langle Enn'_n, Enn'_n \rangle = |\partial_z Enn^1_n|^2 + |\partial_z Enn^2_n|^2 + |\partial_z Enn^3_n|^2 = 0.$$

Following [EJ14, Ch. 8.4], ψ can be reconstructed using the antiderivative, which leads to the fundamental statement that there is (up to a translation) a one-to-one relationship between conformal parameterized minimal surfaces and isotropic, holomorphic functions.

Theorem 11 (Enneper-Weierstrass)**.** *Let $\psi : \mathcal{U} \to \mathbb{R}^3$ be a conformal parameterized minimal surface. Then $2\psi_z$ is an isotropic and holomorphic map. Conversely, for an isotropic, holomorphic $\phi : \mathcal{U} \to \mathbb{C}^3 \setminus \{0\}$ the surface $Re\left(\int \phi\right)$ is a conformal minimal surface. The following applies*

$$\phi = 2\psi_z \text{ and } \psi = Re\left(\int \phi\right). \tag{4.3}$$

Proof. In Theorem 10 the equivalence between conformally parameterized minimal surfaces ψ and it's derivative ψ_z has been established. From this it can also be concluded that the antiderivative of ψ_z is a conformal minimal surface. It remains to show equations (4.3).

Let ψ be a conformal parametrization and $\int \phi$ be the antiderivative of a holomorphic function ϕ. Then ψ is (up to translation) the $Re\left(\int \phi\right)$, i.e., $\psi - Re\left(\int \phi\right)$ is constant. Calculating the Wirtinger derivatives of the last expression yields

$$\begin{aligned}\left(\psi - Re\left(\int \phi\right)\right)_z &= \psi_z - \frac{1}{2}\left(\int \phi + \overline{\int \phi}\right)_z \\ &= \psi_z - \frac{1}{2}\phi \\ &= \psi_z - \psi_z \\ &= 0.\end{aligned}$$

Note that $\left(\overline{\int \phi}\right)_z$ vanishes, since ϕ is holomorphic and $\left(\overline{\int \phi}\right)_z$ is the complex conjugate of $\left(\int \phi\right)_{\bar{z}}$. Analogously, $\left(\psi - Re\left(\int \phi\right)\right)_{\bar{z}}$ is zero and hence, $\psi - Re\left(\int \phi\right)$ is constant. □

If ϕ is holomorphic and isotropic, so $e^{i\theta}\phi$ for $\theta \in [0, 2\pi]$ and hence, a whole family of minimal surfaces, the so-called associated family, is obtained [GAS17, Ch. 22; EJ14, Ch. 8].

Definition 18. *The 1-parameter family*

$$\psi_\theta = Re\left(e^{i\theta}\int \phi\right), \tag{4.4}$$

for $\theta \in [0, 2\pi]$, is denoted as the associated family of ψ.

Using Theorem 11, Weierstrass derived a representation formula for minimal surfaces, which provides an essential method for their generation [EJ14, Ch. 8.5].

Theorem 12 (Weierstrass Representation). *A function $\psi : \mathcal{U} \to \mathbb{R}^3$ with $\psi = Re\left(\int \phi\right)$ and*

$$\phi = f\left(\frac{1}{2}\left(\frac{1}{g} - g\right), -\frac{1}{2i}\left(\frac{1}{g} + g\right), 1\right) \tag{4.5}$$

defines a conformally parameterized minimal surface for any holomorphic function $f : \mathcal{U} \to \mathbb{C}$ and meromorphic function $g : \mathcal{U} \to \mathbb{C}$, such that the components of ϕ do not contain poles and there are no common zeros.

Proof. Let ϕ be holomorphic and isotropic. Theorem 11 implies that $Re\left(\int \phi\right)$ is a conformally parameterized minimal surface. It remains to show Equation (4.5). Therefore, we use the isotropy of $\phi = (\phi^1, \phi^2, \phi^3)$

$$\begin{aligned} 0 &= \langle \phi, \phi \rangle = (\phi^1)^2 + (\phi^2)^2 + (\phi^3)^2 \\ &= (\phi^1)^2 - i^2(\phi^2)^2 + (\phi^3)^2 = (\phi^1 + i\phi^2)(\phi^1 - i\phi^2) + (\phi^3)^2 \end{aligned}$$

Define $f := \phi^3$ and $g := \frac{\phi^3}{(\phi^1 - i\phi^2)}$. Since, ϕ is holomorphic so its components, in particular ϕ^3, and the quotient of two holomorphic functions is meromorphic. Calculation shows

$$(\phi^1 - i\phi^2) = \frac{f}{g}, \ (\phi^1 + i\phi^2) = -fg.$$

Adding and subsequently subtracting both equations yields

$$2\phi^1 = \frac{f}{g} - fg, \ -2i\phi^2 = \frac{f}{g} + fg.$$

□

Remark: There are different conventions on defining f and g in the proof of Theorem 12. In parts of the literature the functions are defined as $f := \phi^1 - i\phi^2$ and $g := \frac{\phi^3}{(\phi^1 - i\phi^2)}$ [GAS17, Ch. 22.5]. A similar calculation leads to the slightly different representation

$$\tilde{\phi} = f\left(\frac{1}{2}\left(1 - g^2\right), -\frac{1}{2i}\left(1 + g^2\right), g\right).$$

4.2 Lie's Construction of Minimal Surfaces as Translation Surfaces

An intuitive and illustrative representation of a minimal surface is that as a translation surface. Lie showed that every minimal surface can be obtained as a translation surface of two generating curves [Lie22, Nit89].

Definition 19. *A surface $\mathcal{S}$ in $\mathbb{R}^3$ is a **translation surface**, if $\mathcal{S}$ can be locally expressed by the sum of two so-called generating curves $\gamma_1 : I \to \mathbb{R}^3$ and $\gamma_2 : J \to \mathbb{R}^3$, i.e., $\psi(u, v) = \gamma_1(u) + \gamma_2(v)$, where $I, J \subset \mathbb{R}$ are intervals [GAS17, Ch. 13].*

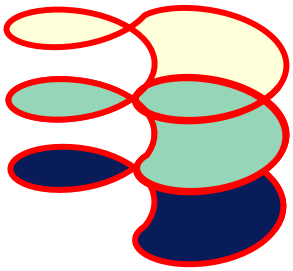

Figure 4.2: Helicoid considered as surface of translation with curves γ_1, γ_2 depicted in red.

Example 7. *The helicoid defined in Equation (2.8) can be re-parameterized using*

$$v = 2\cos\left(\frac{r-s}{2}\right),\ u = \frac{r+s}{2}, \tag{4.6}$$

with new parameters r, s [Nit89, §77]. Inserting (4.6) in (2.8) and sum-to-product identities for trigonometric functions, equations (10.2)-(10.3), yields

$$\begin{aligned} hel &= \left(2\cos\left(\frac{r-s}{2}\right)\cos\left(\frac{r+s}{2}\right), 2\cos\left(\frac{r-s}{2}\right)\sin\left(\frac{r+s}{2}\right), \frac{r+s}{2}\right) \\ &= \left(\cos(r)+\cos(s), \sin(r)+\sin(s), \frac{r}{2}+\frac{s}{2}\right) \\ &= \left(\cos(r), \sin(r), \frac{r}{2}\right) + \left(\cos(s), \sin(s), \frac{s}{2}\right). \end{aligned}$$

Hence, $hel(r,s) = \gamma_1(r) + \gamma_2(s)$ is a translation surface, i.e., the minimal surface is generated by a translation of $\gamma_1(r)$ along the curve $\gamma_2(s)$ (or vice versa), cf. Figure 4.2. This is a special case where the generating curves are real.

Theorem 13. *Every minimal surface is a translation surface of an isotropic curve η and its complex conjugated curve $\bar{\eta}$, i.e., $\psi(u,v) = \eta(z) + \overline{\eta(z)}$. Furthermore, η satisfies $\langle \eta'(z), \eta'(z)\rangle = 0$ and is therefore a minimal curve [Nit89, §148].*

Proof. According to Theorem 11 a conformal parameterized minimal surface $\psi : \mathcal{U} \to \mathbb{R}^3$ is, up to translation (with constant $\psi_0 \in \mathbb{R}^3$), the real part of $\int \phi$. In particular,

$$\begin{aligned} \psi(u,v) &= \psi_0 + Re\left(\int \phi\right) \\ &= \psi_0 + \frac{1}{2}\left(\int \phi + \overline{\int \phi}\right) \\ &= \frac{1}{2}\left(\psi_0 + \int \phi\right) + \frac{1}{2}\left(\psi_0 + \overline{\int \phi}\right) \\ &= \frac{1}{2}\left(\psi_0 + \int \phi\right) + \frac{1}{2}\left(\overline{\psi_0 + \int \phi}\right). \end{aligned}$$

Then $\eta(z) := \frac{1}{2}\left(\psi_0 + \int \phi\right)$ satisfies the isotropy condition $\langle \eta'(z), \eta'(z)\rangle = 0$, since ϕ does, and ψ can be expressed as translation of η and its complex conjugated curve $\bar{\eta}$. □

Example 8. *Scherk's surface can be obtained as graph of a function* $\psi(u,v) = \gamma_1(u) + \gamma_2(v)$*, i.e.,* $x(u,v) = (u,v,\psi(u,v))$*, with vanishing mean curvature [GAS17, Ch. 16.5]. Calculating the derivatives of* x

$$x_u = (1,0,\psi_u)^\intercal\,,\ x_v = (0,1,\psi_v)^\intercal$$
$$x_{uu} = (0,0,\psi_{uu})^\intercal\,,\ x_{uv} = (0,0,\psi_{uv})^\intercal\,,\ x_{vv} = (0,0,\psi_{vv})^\intercal$$

and the normal N

$$N(u,v) = \frac{x_u \times x_v}{||x_u \times x_v||} = \frac{1}{\sqrt{1+\psi_u^2+\psi_v^2}}(-\psi_u,-\psi_v,1)^\intercal\,,$$

according to Lemma 2, the mean curvature can be expressed by

$$H = \frac{(1+\psi_v^2)\psi_{uu} - 2\psi_u\psi_v\psi_{uv} + (1+\psi_u^2)\psi_{vv}}{2(1+\psi_u^2+\psi_v^2)^{\frac{3}{2}}}. \tag{4.7}$$

Since every minimal surface has zero mean curvature (4.7) simplifies to

$$0 = H = (1+\psi_v^2)\psi_{uu} - 2\psi_u\psi_v\psi_{uv} + (1+\psi_u^2)\psi_{vv}, \tag{4.8}$$

which is also called the ***minimal surface equation****. Due to the specific structure of* $\psi = \gamma_1 + \gamma_2$*,*

$$\psi_u = \gamma_1'(u),\ \psi_v = \gamma_2'(v)$$
$$\psi_{uu} = \gamma_1''(u),\ \psi_{uv} = 0,\ \psi_{vv} = \gamma_2''(v)$$

the minimal surface equation becomes

$$0 = (1+\gamma_2'(v)^2)\gamma_1''(u) + (1+\gamma_1'(u)^2)\gamma_2''(v). \tag{4.9}$$

The last Equation (4.9) can be solved by separation of variables,

$$\frac{\gamma_1''(u)}{(1+\gamma_1'(u)^2)} = c = -\frac{\gamma_2''(v)}{(1+\gamma_2'(v)^2)},$$

with some constant c*. Integration yields*

$$\begin{aligned}\gamma_1(u) &= -\frac{1}{c}\log(\cos(cu)+d_1)+d_2,\\ \gamma_2(v) &= \frac{1}{c}\log(\cos(cv+d_3))+d_4,\end{aligned}$$

for some constants d_i*,* $i = 1\ldots4$*. In summary, we obtain* ***Scherk's minimal surface****,*

$$scherk_c(u,v) = \left(u, v, \frac{1}{c}\log\left(\frac{\cos(cv)}{\cos(cu)}\right)\right), \tag{4.10}$$

which is, in case of $c = 1$*, well-defined for all* (u,v) *such that* $\cos(u)\cos(v) > 0$*. The surface is displayed in Figure 4.3.*

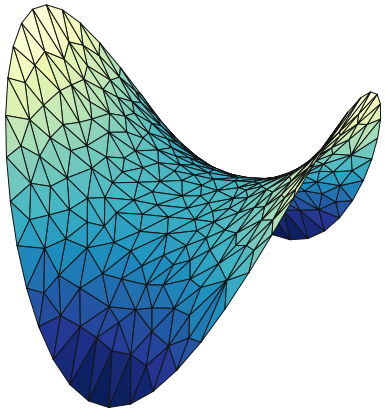

Figure 4.3: Scherk's surface with $c = 1$ and parameter domain $\mathbb{D}$.

5 Björling's Formula

A problem related to that of Plateau is to find a minimal surface containing an analytical strip and was first asked by Björling [Bjö44]. For this problem, there is a formula to generate a minimal surface for a given analytical strip, which we recount from [GAS17, Ch. 22.6] in this chapter. Finally, we introduce the Catalan's surface as an example.

Definition 20. *A **holomorphic extension** of a curve $\gamma : (a, b) \to \mathbb{R}^3$ is a holomorphic function defined on the strip*

$$\mathbb{S} = \{(u + iv) \big| u \in (a, b), v \in (c, d), c < 0 < d\}$$

such that the extension coincides with $\gamma(u)$ for $u \in (a, b)$.

Definition 21. *Assuming that there exists a holomorphic extension to the strip $\mathbb{S}$ of two curves $\gamma, \eta : (a, b) \to \mathbb{R}^3$ satisfying*

$$||\eta|| = 1, \ \langle \gamma', \eta \rangle = 0 \tag{5.1}$$

*for $z \in \mathbb{S}$, the **Björling curve** for γ and η is defined as*

$$\beta_{\gamma,\eta}(z) = \gamma(z) - i \int_{z_0}^{z} \eta(z) \times \gamma'(z) dz, \tag{5.2}$$

for some arbitrary, fixed z_0.

Theorem 14. *The mapping $\beta_{\gamma,\eta}(z)$ defines a minimal curve and $\eta(u) = N(u, 0)$, where N is the unit normal to $Re(\beta_{\gamma,\eta}(u + iv))$ with $z = u + iv$.*

Proof. First, calculate the inner product

$$\begin{aligned} \langle \beta'_{\gamma,\eta}, \beta'_{\gamma,\eta} \rangle &= \langle \gamma' - i\eta \times \gamma', \gamma' - i\eta \times \gamma' \rangle \\ &= \langle \gamma', \gamma' \rangle - \langle \eta \times \gamma', \eta \times \gamma' \rangle - 2i \langle \gamma', \eta \times \gamma' \rangle. \end{aligned}$$

Since $\eta \times \gamma'$ is orthogonal to γ', the last term vanishes. Further, applying the identity $||a \times b||^2 = ||a||^2 ||b||^2 - |\langle a, \bar{b} \rangle|^2$ for $a, b \in \mathbb{C}$, yields

$$\langle \beta'_{\gamma,\eta}, \beta'_{\gamma,\eta} \rangle = \langle \gamma', \gamma' \rangle - \langle \eta, \eta \rangle \langle \gamma', \gamma' \rangle + |\langle \eta, \bar{\gamma}' \rangle|^2.$$

The function γ has values in $\mathbb{R}^3$ and Equation (5.1) holds, so $\langle \beta'_{\gamma,\eta}, \beta'_{\gamma,\eta} \rangle = 0$ and $\beta_{\gamma,\eta}$ is a minimal curve.

A calculation similar to the first one, shows $\langle \beta'_{\gamma,\eta}, \overline{\beta'}_{\gamma,\eta} \rangle = 2\langle \gamma', \gamma' \rangle$ and by using further algebraic properties of the cross product

$$\begin{aligned} \beta'_{\gamma,\eta} \times \overline{\beta'}_{\gamma,\eta} &= \gamma' \times \gamma' + \gamma' \times (i\eta \times \gamma') - \gamma' \times (\gamma' \times i\eta) - (\gamma' \times i\eta) \times (\gamma' \times i\eta) \\ &= 2(\gamma' \times (i\eta \times \gamma')) = 2(\langle \gamma', \gamma' \rangle i\eta - i \langle \gamma', \eta \rangle \gamma') \\ &= 2(\langle \gamma', \gamma' \rangle i\eta. \end{aligned}$$

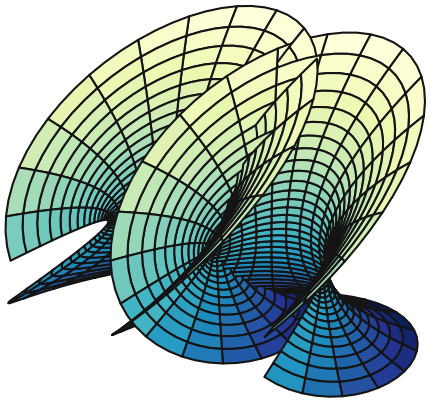

Figure 5.1: Catalan's minimal surface.

This results in the following unit normal field

$$N(u,0) \quad = \quad \frac{\beta'_{\gamma,\eta} \times \overline{\beta'}_{\gamma,\eta}}{i\langle \beta'_{\gamma,\eta}, \overline{\beta'}_{\gamma,\eta}\rangle} = \frac{2\langle \gamma', \gamma'\rangle i\eta}{2i\langle \gamma', \gamma'\rangle} = \eta(u),$$

which proves the second statement. □

For a regular plane curve with a holomorphic extension $\gamma : \mathbb{S} \to \mathbb{C}^2$, Equation (5.2) can be simplified to

$$\beta_\gamma(z) = \left(\gamma_1(z), \gamma_2(z), i\int_{z_0}^{z} \sqrt{\gamma_1'(z)^2 + \gamma_2'(z)^2}dz\right), \tag{5.3}$$

where $\gamma = (\gamma_1, \gamma_2)$ are the components of γ.

Theorem 15. *Let $\gamma : (a,b) \to \mathbb{R}^2$ be a plane curve with $||\gamma'(t)|| = 1$ for $a < t < b$. Assuming that there is a holomorphic extension to γ on $\mathbb{S}$, the $Re(\beta_\gamma)$ is a minimal surface, which has γ as a geodesic.*

Example 9. *The surface with $\gamma(t) = (t - \sin(t), 1 - \cos(t))$ as geodesic, obtained by Theorem 15, is called Catalan's minimal surface, cf. Figure 5.1.*

6 New Minimal Surfaces from Old Minimal Surfaces

A novel approach of generating minimal surfaces from known ones using complex projective geometry and Theorem 11 is presented. We show that for a certain class, namely algebraic minimal surfaces, our construction yields again a minimal surface in an appropriate neighborhood.

Let ψ_1, ψ_2, and $\psi_3 : \mathbb{C} \to (\mathbb{C} \cup \{\infty\})^3 =: \hat{\mathbb{C}}^3$ be three different minimal curves and ψ_i^j, $i = 1, 2, 3$, denote the j-th component of ψ_i. By Definition 17 the derivatives of the functions ψ_i, $i = 1, 2, 3$, are isotropic, i.e., for all z

$$0 = \langle \psi_i'(z), \psi_i'(z) \rangle = \left(\partial_z \psi_i^1\right)^2 + \left(\partial_z \psi_i^2\right)^2 + \left(\partial_z \psi_i^3\right)^2.$$

Let $C := \{f : \mathbb{C} \to \hat{\mathbb{C}}^3 \big| f^i \text{ holomorphic}\}$ denote the set of three-dimensional maps with holomorphic components. Then minimal curves can be identified as points on a quadric

$$q := \{x \in C^3 | \, \langle x, x \rangle = 0\},$$

which is a cone, cf. Figure 6.1. Now, considering the plane in C^3 spanned by ψ_1', ψ_2' and ψ_3', our goal is to examine the conic section with q. For this purpose, homogeneous coordinates are used. In particular, the following embedding into C^4 is considered

$$\begin{aligned} \hat{} : C^3 &\to C^4 \\ z = (z_1, z_2, z_3) &\mapsto (1, z_1, z_2, z_3) =: \hat{z} \end{aligned}$$

and $[\hat{z}] = \{\lambda \hat{z} \in C^4 \mid \lambda \in \mathbb{C}\}$ denote the corresponding homogeneous coordinates in $\mathcal{P}^3 = \{[\hat{z}] \mid z \in C^4 \setminus \{0\}\}$. In line with this, we define

$$\tilde{\psi}_1 := (1, \psi_1'), \tilde{\psi}_2 := (1, \psi_2'), \tilde{\psi}_3 := (1, \psi_3')$$

and

$$\tilde{\Psi}_1 := [\tilde{\psi}_1], \tilde{\Psi}_2 := [\tilde{\psi}_2], \tilde{\Psi}_3 := [\tilde{\psi}_3]$$

as the homogenized coordinates in $\mathcal{P}^3$. Next, the conic section with the projective quadric

$$Q = \{[z_0, z_1, z_2, z_3] \in \mathcal{P}^3 \mid z_1^2 + z_2^2 + z_3^2 = 0\}$$

is calculated. Therefore, consider the plane $\mathcal{E}$ spanned by the embedded derivatives $\tilde{\Psi}_1, \tilde{\Psi}_2$ and $\tilde{\Psi}_3$ of minimal curves in $\mathcal{P}^3$,

$$\alpha \tilde{\psi}_1 + \beta \tilde{\psi}_2 + \gamma \tilde{\psi}_3, \tag{6.1}$$

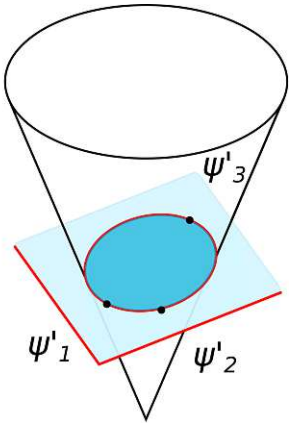

Figure 6.1: Cone q.

with $\alpha, \beta, \gamma \in \mathbb{R} \setminus \{0\}$ and calculate the intersections with the cone,

$$0 = \langle \alpha\tilde{\psi}_1 + \beta\tilde{\psi}_2 + \gamma\tilde{\psi}_3, \alpha\tilde{\psi}_1 + \beta\tilde{\psi}_2 + \gamma\tilde{\psi}_3 \rangle_{\mathcal{P}^3}. \tag{6.2}$$

We further expand Equation (6.2) to

$$0 = \alpha^2\langle\tilde{\psi}_1, \tilde{\psi}_1\rangle_{\mathcal{P}^3} + \alpha\beta\langle\tilde{\psi}_1, \tilde{\psi}_2\rangle_{\mathcal{P}^3} + \alpha\gamma\langle\tilde{\psi}_1, \tilde{\psi}_3\rangle_{\mathcal{P}^3} + \beta\alpha\langle\tilde{\psi}_2, \tilde{\psi}_1\rangle_{\mathcal{P}^3} + \tag{6.3}$$

$$\cdots + \gamma\beta\langle\tilde{\psi}_3, \tilde{\psi}_2\rangle_{\mathcal{P}^3} + \gamma^2\langle\tilde{\psi}_3, \tilde{\psi}_3\rangle_{\mathcal{P}^3}. \tag{6.4}$$

Exploiting the symmetry of the inner product on $\mathcal{P}^3$ and the fact that $\langle\tilde{\psi}_i, \tilde{\psi}_i\rangle_{\mathcal{P}^3} = 0$ (due to the isotropy condition satisfied by minimal curves), the equations (6.3)-(6.4) can be further simplified to

$$0 = 2\alpha\beta\langle\tilde{\psi}_1, \tilde{\psi}_2\rangle_{\mathcal{P}^3} + 2\alpha\gamma\langle\tilde{\psi}_1, \tilde{\psi}_3\rangle_{\mathcal{P}^3} + 2\beta\gamma\langle\tilde{\psi}_2, \tilde{\psi}_3\rangle_{\mathcal{P}^3}. \tag{6.5}$$

Hence, we can express γ in terms of α and β

$$\gamma = -\frac{\alpha\beta\langle\tilde{\psi}_1, \tilde{\psi}_2\rangle_{\mathcal{P}^3}}{\alpha\langle\tilde{\psi}_1, \tilde{\psi}_3\rangle_{\mathcal{P}^3} + \beta\langle\tilde{\psi}_2, \tilde{\psi}_3\rangle_{\mathcal{P}^3}} \tag{6.6}$$

and using this representation in Equation (6.1) yields

$$\frac{\alpha^2\langle\tilde{\psi}_1, \tilde{\psi}_3\rangle_{\mathcal{P}^3}\tilde{\psi}_1 + \alpha\beta\left(\langle\tilde{\psi}_2, \tilde{\psi}_3\rangle_{\mathcal{P}^3}\tilde{\psi}_1 + \langle\tilde{\psi}_1, \tilde{\psi}_3\rangle_{\mathcal{P}^3}\tilde{\psi}_2 - \langle\tilde{\psi}_1, \tilde{\psi}_2\rangle_{\mathcal{P}^3}\tilde{\psi}_3\right) + \beta^2\langle\tilde{\psi}_2, \tilde{\psi}_3\rangle_{\mathcal{P}^3}\tilde{\psi}_2}{\alpha\langle\tilde{\psi}_1, \tilde{\psi}_3\rangle_{\mathcal{P}^3} + \beta\langle\tilde{\psi}_2, \tilde{\psi}_3\rangle_{\mathcal{P}^3}} \tag{6.7}$$

Equation (6.7) describes the conic section of $\mathcal{E}$ and Q in $\mathcal{P}^3$ with homogeneous parameter $(\alpha, \beta) \in \mathbb{R}^2 \setminus \{0\}$. Where we write $c(\alpha, \beta)$ hereafter as abbreviation of (6.7). Note that common multiples of α and β are negligible in projective geometry. Furthermore, (6.7) implies the following findings about the associated family of minimal surfaces.

Lemma 11. *The minimal surfaces of an associated family belong to the rulings of the cone q.*

Proof. Let ψ_1, ψ_2 and ψ_3 be minimal curves of the same associated family of $\tilde{\psi_0}$, i.e.,

$$\psi_1 = e^{i\theta_1}\tilde{\psi_0},\ \psi_2 = e^{i\theta_2}\tilde{\psi_0},\ \psi_3 = e^{i\theta_3}\tilde{\psi_0},$$

with $\theta_k \in [0, 2\pi]$ for $k = 1, \dots, 3$ and θ_k pairwise different. Then for $k \neq l$

$$\langle \psi_k, \psi_l \rangle_{\mathcal{P}^3} = e^{i\theta_k} e^{i\theta_l} \langle \tilde{\psi_0}, \tilde{\psi_0} \rangle_{\mathcal{P}^3} = 0.$$

□

Using dehomogenization of the C^4-valued function $c(\alpha, \beta) = (c_1, c_2, c_3, c_4)$ yields

$$\left(\frac{c_2}{c_1}, \frac{c_3}{c_1}, \frac{c_4}{c_1}\right) =: h, \tag{6.8}$$

where the function $h : \mathbb{C} \to \mathbb{C}^3$ is by construction isotropic. The aim is to derive a minimal surface from h. For this purpose, we would like use Theorem 11, but in general it is not known whether h is holomorphic in some neighborhood $\mathcal{U}$ and it potentially contains poles. However, for a certain class of functions, namely *algebraic minimal curves*, h is meromorphic.

Definition 22. *A minimal curve $\psi : \mathcal{U} \to \mathbb{C}^n$, where ψ is an algebraic function, i.e., there is an irreducible polynomial P in two variables and coefficients in $\mathbb{C}$ such that*

$$P(\psi(z), z) = 0$$

is called algebraic minimal curve.

Example 10. *The Enneper's minimal curves Enn_n are rational functions and hence, algebraic minimal curves.*

Lemma 12. *Let ψ_1, ψ_2, and $\psi_3 : \mathbb{C} \to \hat{\mathbb{C}}$ be algebraic minimal curves. Then the conic section h defined by Equation (6.7) is meromorphic.*

Proof. Since h is rational in each component and rational functions are meromorphic, cf. Example 3. □

Let's restrain to the case of algebraic minimal curves ψ_1, ψ_2, ψ_3 and let $\mathcal{U} \subseteq \mathbb{C}$ be open, connected and such that h has no poles in it. Then by Theorem 11 the real part $Re\left(\int h\right)$ is a conformal parameterized minimal surface for any parameters α, β. We summarize our findings in the following theorem.

Theorem 16. *Let ψ_1, ψ_2 and $\psi_3 : \mathbb{C} \to \hat{\mathbb{C}}$ be algebraic minimal curves, not belonging to the same associated family. Then*

- $\tilde{\Psi}_1 := [(1, \psi_1')], \tilde{\Psi}_2 := [(1, \psi_2')], \tilde{\Psi}_3 := [(1, \psi_3')] \in Q$
- *there is a parametrization of the conic section $\mathcal{E} \cup Q$ and an open, connected neighborhood $\mathcal{U} \subseteq \mathbb{C}$ such that $h : \mathcal{U} \to \mathbb{C}^3$ defined in (6.8) is a complex-valued holomorphic, isotropic function for any α, β and*
- *$Re\left(\int h\right)$ is a conformal parameterized minimal surface.*

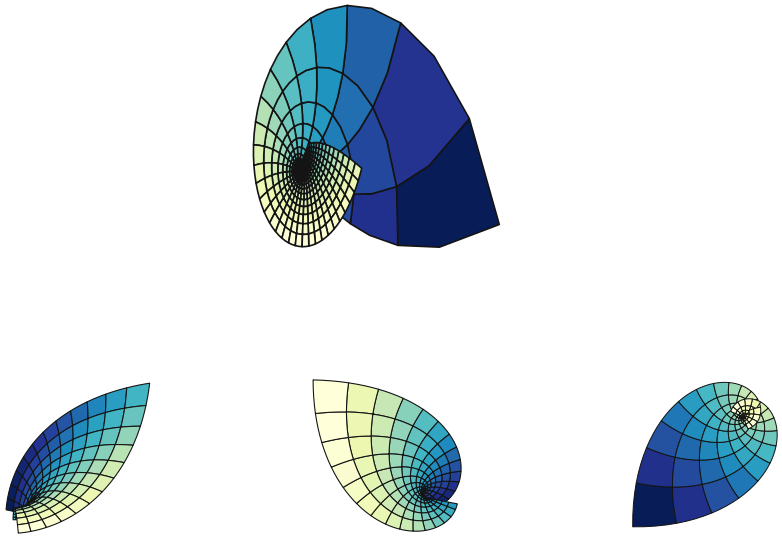

Figure 6.2: Enneper's minimal surfaces with degree 1,2,3 (bottom, f.l.t.r.) and the obtained minimal surface by our construction (top) in the parameter domain $[-1.9 : -0.1] \times [-1.9 : -0.1]$ looking in the xy-plane.

6.1 Experiments with three Minimal Curves

Using the approach presented above we explore the obtained surfaces.

Example 11. *As a first example we construct function h, as described in Theorem 16, using the three algebraic minimal surfaces $\psi_1 = Enn_1, \psi_2 = Enn_2$ and $\psi_3 = Enn_3$ with parameter $\alpha = -2$ and $\beta = 1$. This results in*

$$h = \left(\frac{-z^6+4z^5-8z^3-3z^2+4z+4}{z^2+4z+4}, \frac{i(z^6-4z^5+8z^3+5z^2+4z+4)}{z^2+4z+4}, \frac{2z(-z^2+2z+2)}{z+2} \right).$$

Python's `sympy` *library detects three isolated singularities: $\{-2, 0, 1\}$. Therefore, we choose $\mathcal{U}$ as the region bounded by $[-1.9 : -0.1] \times [-1.9 : -0.1]$. Within this neighborhood h is holomorphic and $Re\left(\int h\right)$ is an algebraic minimal surface. Compare Figure 6.2.*

The requirement of a holomorphic f in Theorem 12 is often too restrictive. There are several examples of minimal surfaces, where f has isolated singularities. One famous example originating back in 1876 is the Henneberg surface [Hen75; Hen76; GAS17, Ch. 22.5].

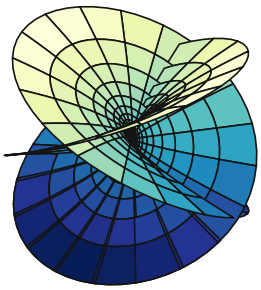

Figure 6.3: Henneberg minimal surface.

Example 12. *Consider the Weierstrass representation of the Henneberg minimal surface, Figure 6.3, generated with* $f(z) = (\frac{z^4-1}{z^3})$ *and* $g(z) = z$ *in Theorem 12*

$$henneberg(z) : \begin{cases} \mathbb{C} \to \mathbb{C}^3 \\ z \mapsto (1 - \frac{1}{z^4}) \left(\frac{1}{2}(1 - z^2), -\frac{1}{2i}(1 + z^2), z\right). \end{cases}$$

This function f *has a pole of order 3 at* $z_0 = 0$.

Following this example, we extend the neighborhood in Example 11, where the parameters α, β are maintained unchanged and examine the obtained figures with meromorphic h and a symmetric neighborhood $\mathcal{U} = [-1 : 1] \times [-1 : 1]$. The resulting surface is displayed in Figure 6.4.

Next, we modify the parameters α, β and explore the resulting figure in a further extended neighborhood that contains all poles of the function h.

Example 13. *In order to construct the function* h*, the first three Enneper's minimal surfaces* $\psi_1 = Enn_1, \psi_2 = Enn_2$ *and* $\psi_3 = Enn_3$ *are used. We choose the parameters* $\alpha = 2$ *and* $\beta = 1$ *and use Python's* `sympy` *to derive the integrand*

$$h = \left(\frac{-z^6-4z^5-8z^4-8z^3+5z^2+12z+4}{9z^2+12z+4}, \frac{i(z^6+4z^5+8z^4+8z^3+13z^2+12z+4)}{9z^2+12z+4}, \frac{2z(z^2+2z+2)}{3z+2}\right).$$

The complex-valued function h *has three poles* $\{-\frac{2}{3}, 0, 1\}$*. We explore the figure obtained in an neighborhood* $\mathcal{U} = [-4 : 4] \times [-4 : 4]$ *containing all isolated singularities. The obtained surface is depicted in Figure 6.5.*

Due to the observation in Example 13, we vary the parameters α and β along the conic section and examine their effects on the resulting surfaces.

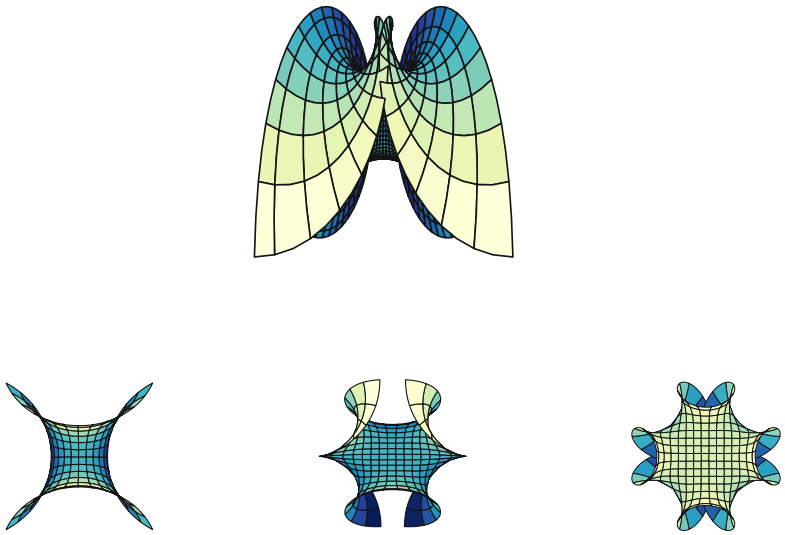

Figure 6.4: Constructed surface with parameter $\alpha = -2$ and $\beta = 1$ (top) in the extended neighborhood $[-1 : 1] \times [-1 : 1]$ with Enneper's minimal surfaces with degree 1,2,3 (bottom) as initial curves. Represented in the xy-plane.

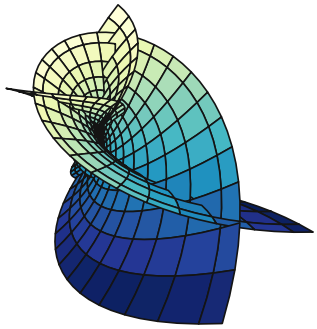

Figure 6.5: Surface obtained from initial minimal curves $\psi_1 = Enn_1, \psi_2 = Enn_2$ and $\psi_3 = Enn_3$ with parameter $\alpha = 2$ and $\beta = 1$ depicted in the neighborhood $[-4 : 4] \times [-4 : 4]$, where h has three poles $\{-\frac{2}{3}, 0, 1\}$.

Example 14. *Again, we consider the first three Enneper's minimal surfaces $\psi_1 = Enn_1$, $\psi_2 = Enn_2$ and $\psi_3 = Enn_3$ in a neighborhood $\mathcal{U} = [-4 : 4] \times [-4 : 4]$ that may contain poles of the resulting function $h(\alpha, \beta, z)$ and vary the parameters α, β. Setting $\alpha = 10, \beta = 0$ results in (scaled) Enn_1 and vice versa Enn_2. Parameter combinations in-between display a transformation from one minimal surface into another, cf. Figure 6.6.*

This immediate consequence of the construction indicated above outlines one possible usage, the deformation of a minimal surface into another one, similarly to Theorem 1.

Corollary 3. *Let ψ_1 and ψ_2 be two different algebraic minimal surfaces and $T(\alpha, \beta)(z) := Re\left(\int h(\alpha, \beta, z)\right)$, where h satisfies Equation 6.8. Then T describes a deformation between minimal surface $\psi_1 = T(1, 0)(z)$ and $\psi_2 = T(0, 1)(z)$. $T(\alpha, \beta)(z)$ is minimal for each α, β in a neighborhood $\mathcal{U}$, where $h|_{\mathcal{U}}$ is holomorphic.*

Proof. Consider Theorem 16 with an arbitrary ψ_3. □

6.2 Experiments with other Planes

In the previous sections we considered the conic section of a plane spanned by three pairwise different minimal curves embedded in $\mathcal{P}^3$ with a quadric in order to obtain a new minimal surface. Based on this construction we further examine the conic section with planes spanned by just two minimal curves and some arbitrary additional point, in complex projective space.

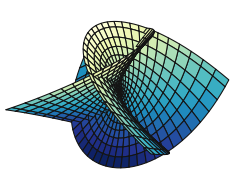

(a) $\alpha = 10$, $\beta = 0$

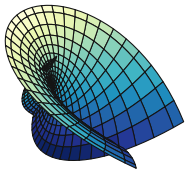

(b) $\alpha = 9$, $\beta = 1$

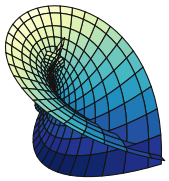

(c) $\alpha = 8$, $\beta = 2$

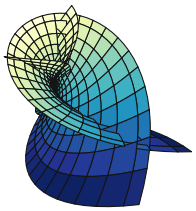

(d) $\alpha = 7$, $\beta = 3$

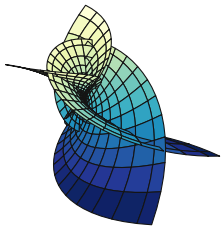

(e) $\alpha = 6$, $\beta = 4$

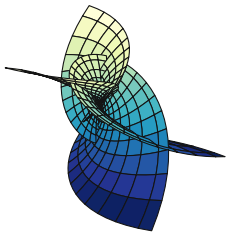

(f) $\alpha = 5$, $\beta = 5$

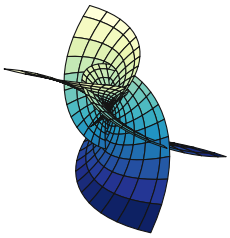

(g) $\alpha = 4$, $\beta = 6$

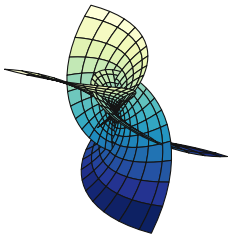

(h) $\alpha = 3$, $\beta = 7$

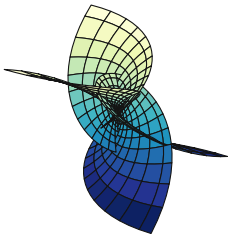

(i) $\alpha = 2$, $\beta = 8$

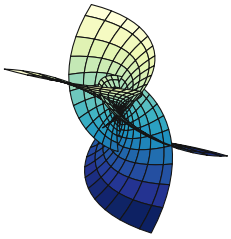

(j) $\alpha = 1$, $\beta = 9$

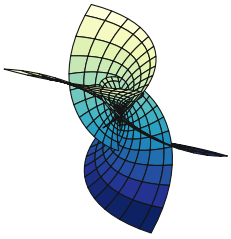

(k) $\alpha = 0$, $\beta = 10$

Figure 6.6: Varying the parameters α and β in the range $[0, 10]$ with step-size 1 describes a deformation of Enn_1 to Enn_2 minimal surface.

Example 15. *Now, with the intention to cut the quadric q with a plane spanned by two minimal curves and one additional point, we utilize the settings $\psi_1 = Enn_1$, $\psi_2 = Enn_2$ and vary $\tilde{\Psi}_3 \in \mathcal{P}^3$ in positive and negative x-direction. We choose $\tilde{\Psi}_3 \in \{(1,-3,0,0),(1,1,0,0),(1,1.7,0,0),(1,3,0,0)\}$ and set the parameters $\alpha = 9, \beta = 90$. In order to evaluate the integral on a triangulated grid, we use numerical integration, cf. Chapter 7. We observe that a larger x-value stretches the surface, cf. Figure 6.7b-6.7d, and for $x = 3$ or $\tilde{\Psi}_3 = (1,3,0,0)$ the upper intersection disappears, Figure 6.7d. Furthermore, changing the sign of the x-value in $\tilde{\Psi}_3$ yields a rotated figure, in this particular case, the mirrored surface along the yz-plane, cf. Figure 6.7a and Figure 6.7d.*

Example 16. *Let ψ_1, ψ_2 be as in Example 15, but instead we choose $\alpha = 54, \beta = 45$ and survey the influence of the choice of $\tilde{\Psi}_3$ in various directions, in particular, the yz-values are combined and changed by ± 1. The results are represented in Figure 6.8. Again, we observe that a changed sign of any xyz-value eventuates in a rotation of the object. For example, Figure 6.8a is Figure 6.8g rotated by $\frac{\pi}{2}$ in xz-direction. Noticeable is the surface obtained by setting $\tilde{\Psi}_3 = (1,0,0,1)$ respectively the rotated counterpart $\tilde{\Psi}_3 = (1,0,0,-1)$, which seems to be neither the result of a rotation nor stretching of the origin surface, cf. Figure 6.8d and Figure 6.8f. Moreover, a comparison of the first and last row in Figure 6.8 shows that the choice of a non-zero z-value has a negligible impact on the generated surface in these cases. Using fixed points $\tilde{\Psi}_3$ such that the relation $x : y \neq 1$, leads to deformations of the initial surface, which is illustrated in Figure 6.10.*

These two examples, confirm the usage of a fixed point $\tilde{\Psi}_3$ in our construction and indicate the influence of a changed sign in the choice of $\tilde{\Psi}_3$, which describes a rotation of the resulting surface.

In the next experiment, we interchange the roles of the two minimal curves $\psi_1 = Enn_1$, $\psi_2 = Enn_2$ and the fixed point $\tilde{\Psi}_3$.

Example 17. *So far, we fixed $\tilde{\Psi}_3$ and set $\psi_1 = Enn_1, \psi_2 = Enn_2$. In this example, we first choose $\tilde{\Psi}_1 = (1,3,0,0)$ fixed and $\psi_2 = Enn_1, \psi_3 = Enn_2$ in (6.7). Afterwards, we fix the second argument $\tilde{\Psi}_2$ setting $\psi_1 = Enn_1, \psi_3 = Enn_2$ and in the end analogously we fix $\tilde{\Psi}_3$, cf. Figure 6.9. This leads to significantly different surfaces, however, exchanging α with β and simultaneously $\tilde{\psi}_2$ with $\tilde{\psi}_2$ yields exactly the same surface as depicted in Figure 6.7d (compared to Figure 6.9c).*

We summarize our findings in Corollary 4.

Corollary 4. *The construction is $(\alpha, \tilde{\psi}_1) - (\beta, \tilde{\psi}_2)$-symmetric, i.e., $c(\alpha, \beta, \tilde{\psi}_1, \tilde{\psi}_2, \tilde{\psi}_3) = c(\beta, \alpha, \tilde{\psi}_2, \tilde{\psi}_1, \tilde{\psi}_3)$.*

Proof. Simple calculation and the symmetry of the inner product. According to (6.7), we have

$$c(\alpha, \beta, \tilde{\psi}_1, \tilde{\psi}_2, \tilde{\psi}_3) = \frac{\alpha^2 \langle \tilde{\psi}_1, \tilde{\psi}_3 \rangle_{\mathcal{P}^3} \tilde{\psi}_1 + \alpha\beta \left(\langle \tilde{\psi}_2, \tilde{\psi}_3 \rangle_{\mathcal{P}^3} \tilde{\psi}_1 + \langle \tilde{\psi}_1, \tilde{\psi}_3 \rangle_{\mathcal{P}^3} \tilde{\psi}_2 - \langle \tilde{\psi}_1, \tilde{\psi}_2 \rangle_{\mathcal{P}^3} \tilde{\psi}_3 \right) + \beta^2 \langle \tilde{\psi}_2, \tilde{\psi}_3 \rangle_{\mathcal{P}^3} \tilde{\psi}_2}{\alpha \langle \tilde{\psi}_1, \tilde{\psi}_3 \rangle_{\mathcal{P}^3} + \beta \langle \tilde{\psi}_2, \tilde{\psi}_3 \rangle_{\mathcal{P}^3}}.$$

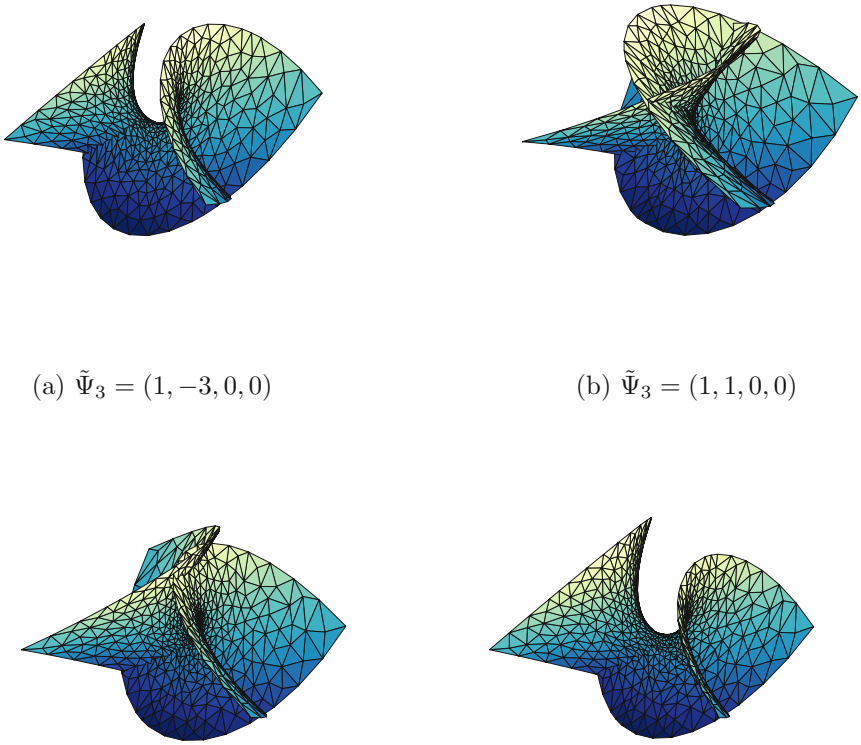

(a) $\tilde{\Psi}_3 = (1, -3, 0, 0)$ (b) $\tilde{\Psi}_3 = (1, 1, 0, 0)$

(c) $\tilde{\Psi}_3 = (1, 1.7, 0, 0)$ (d) $\tilde{\Psi}_3 = (1, 3, 0, 0)$

Figure 6.7: Influence of the choice of a fixed point $\tilde{\Psi}_3$ in x-direction with parameter $\alpha = 9$, $\beta = 90$ and $\psi_1 = Enn_1$, $\psi_2 = Enn_2$.

$$c(\beta,\alpha,\tilde{\psi}_2,\tilde{\psi}_1,\tilde{\psi}_3) = \frac{\beta^2\langle\tilde{\psi}_2,\tilde{\psi}_3\rangle_{\mathcal{P}^3}\tilde{\psi}_2+\beta\alpha\left(\langle\tilde{\psi}_1,\tilde{\psi}_3\rangle_{\mathcal{P}^3}\tilde{\psi}_2+\langle\tilde{\psi}_2,\tilde{\psi}_3\rangle_{\mathcal{P}^3}\tilde{\psi}_1-\langle\tilde{\psi}_2,\tilde{\psi}_1\rangle_{\mathcal{P}^3}\tilde{\psi}_3\right)+\alpha^2\langle\tilde{\psi}_1,\tilde{\psi}_3\rangle_{\mathcal{P}^3}\tilde{\psi}_1}{\beta\langle\tilde{\psi}_2,\tilde{\psi}_3\rangle_{\mathcal{P}^3}+\alpha\langle\tilde{\psi}_1,\tilde{\psi}_3\rangle_{\mathcal{P}^3}}.$$

□

The following example shows how to deform a given minimal surface using our approach described at the beginning of this chapter with two fixed points $\tilde{\Psi}_i$, $i \in \{1,2,3\}$.

Example 18. *Consider, for example,* $\psi_1 = Enn_1$ *and fix* $\tilde{\Psi}_2 = (1,0,1,20), \tilde{\Psi}_3 = (1,1,0,0)$ *in projective space* $\mathcal{P}^3$*, where the parameters* α *and* β *are varied such that their sum always equals* 99*. The deformation of the* Enn_1*-surface is illustrated in Figure 6.11. Since we considered an algebraic minimal surface, the generated surfaces have finitely many poles and every resulting object is at least in a neighborhood without poles minimal. The surfaces are depicted in the parameter area* $\mathcal{V} = [-4:4]\times[-4:4]$*. For example, in the case* $\alpha = 54, \beta = 45$*, the integrand* h *has one singularity in* $(0.0548, 0.0249) \in \mathcal{V}$*.*

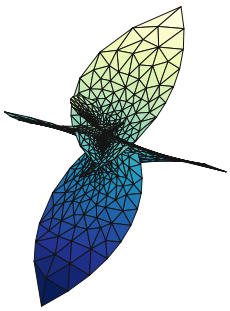

(a) $\tilde{\Psi}_3 = (1, 0, -1, -1)$

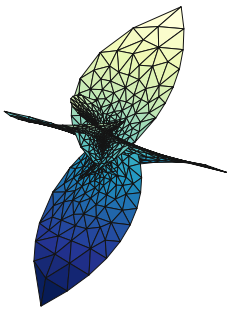

(b) $\tilde{\Psi}_3 = (1, 0, -1, 0)$

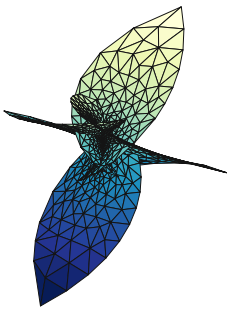

(c) $\tilde{\Psi}_3 = (1, 0, -1, 1)$

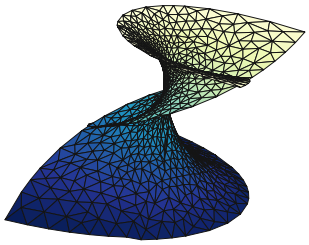

(d) $\tilde{\Psi}_3 = (1, 0, 0, -1)$

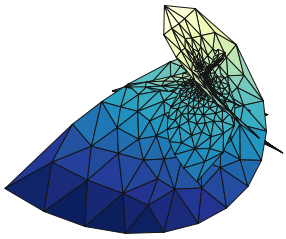

(e) $\tilde{\Psi}_3 = (1, 1, 0, 0)$

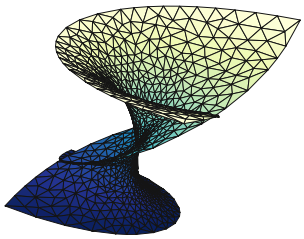

(f) $\tilde{\Psi}_3 = (1, 0, 0, 1)$

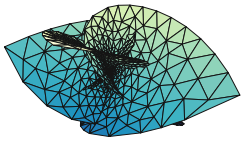

(g) $\tilde{\Psi}_3 = (1, 0, 1, -1)$

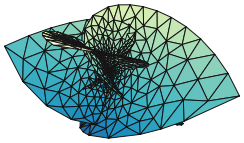

(h) $\tilde{\Psi}_3 = (1, 0, 1, 0)$

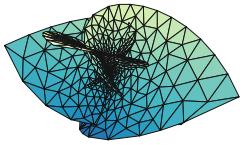

(i) $\tilde{\Psi}_3 = (1, 0, 1, 1)$

Figure 6.8: Influence of the choice of one fixed point $\tilde{\Psi}_3$ with settings $\psi_1 = Enn_1$ and $\psi_2 = Enn_2$ as well as $\alpha = 54, \beta = 45$.

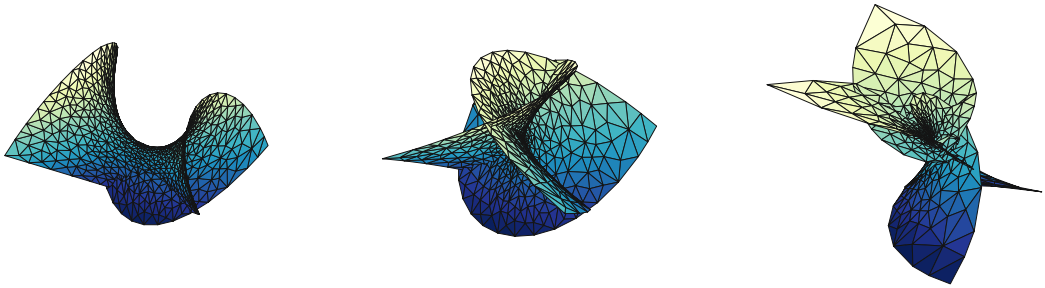

(a) $\tilde{\Psi}_1, \psi_2 = Enn_1, \psi_3 = Enn_2$ (b) $\psi_1 = Enn_1, \tilde{\Psi}_2, \psi_3 = Enn_2$ (c) $\psi_1 = Enn_1, \psi_2 = Enn_2, \tilde{\Psi}_3$

Figure 6.9: Interchanging the roles of the fixed point and the minimal curves Enn_1, Enn_2 in the conic section, where $\tilde{\Psi}_i = (1, 3, 0, 0)$ for $i = 1, 2, 3$, where $\alpha = 90$ and $\beta = 9$.

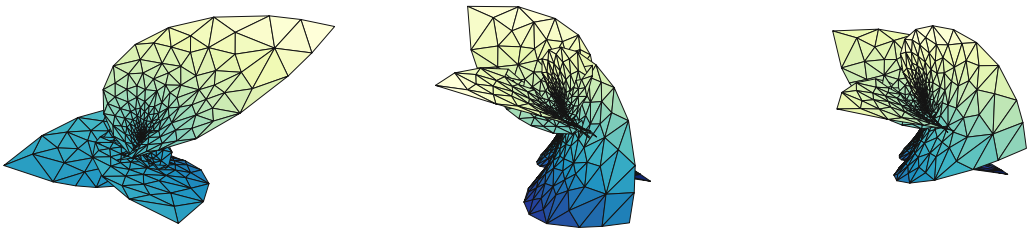

(a) $\tilde{\Psi}_3 = (1, 1, 1, 0)$ (b) $\tilde{\Psi}_3 = (1, 3, 1, 0)$ (c) $\tilde{\Psi}_3 = (1, 1, 3, 0)$

Figure 6.10: Further surfaces with one fixed point $\tilde{\Psi}_3$ and $\psi_1 = Enn_1, \psi_2 = Enn_2$ with parameters $\alpha = 90, \beta = 9$.

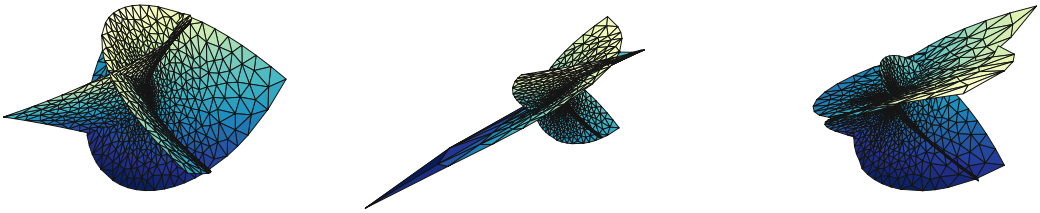

(a) $\alpha = 99$, $\beta = 0$ (b) $\alpha = 90$, $\beta = 9$ (c) $\alpha = 81$, $\beta = 18$

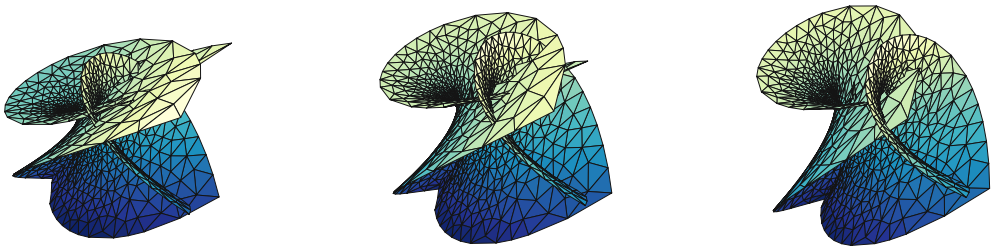

(d) $\alpha = 72$, $\beta = 27$ (e) $\alpha = 63$, $\beta = 36$ (f) $\alpha = 54$, $\beta = 45$

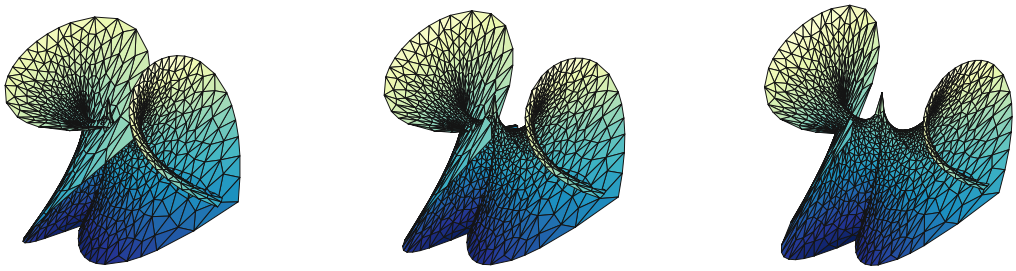

(g) $\alpha = 45$, $\beta = 54$ (h) $\alpha = 36$, $\beta = 63$ (i) $\alpha = 27$, $\beta = 72$

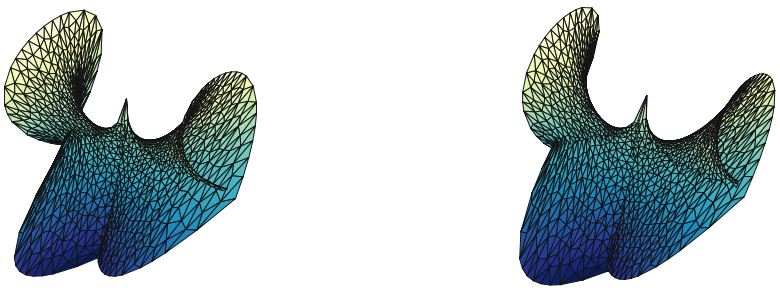

(j) $\alpha = 18$, $\beta = 81$ (k) $\alpha = 9$, $\beta = 90$

Figure 6.11: Varying the parameters α and β in the range $[0, 99]$ describes a deformation of Enn_1 using two fixed points $(1, 0, 1, 20)$ and $(1, 1, 0, 0)$.

7 Numerical Generation

In Chapter 6 several examples of newly generated surfaces were presented. All of these examples had an algebraic integrand and so their antiderivative could be efficiently computed using computer algebra systems like Python's `sympy` library. Nevertheless, we additionally aim for integrands containing analytic functions, e.g., consider a catenoid in Equation (6.7) resp. Equation (6.8) as a starting point. In order to compute the integral in Theorem 16, numerical methods need to be considered. Thereby an adaptive method is preferable, since the integrand might contain singularities.

Let $h : \mathcal{U} \to \mathbb{C}^3$ be the representation of the new minimal curve regarding Chapter 6, Equation (6.8). First, assume h is holomorphic in a simply connected domain $\mathcal{U} \subseteq \mathbb{C}$. Then the integral in Theorem 16 is path-independent. Additionally, let γ be a $\mathcal{C}^1$-curve defined as

$$\begin{aligned} \gamma : [-1,1] &\to \mathcal{U} \\ s &\mapsto \frac{(\mu+\nu)+s(\nu-\mu)}{2}, \end{aligned}$$

the straight line connecting μ and $\nu \in \mathcal{U}$. Further, let H denote the antiderivative of the complex vector-valued function h. Then by chain rule and the fundamental theorem of calculus, the following applies for the i-th, $i = 1, \dots, 3$, component of h

$$\int_\gamma h_i(\omega)d\omega = \int_{-1}^{1} h_i(\gamma(s))\gamma'(s)ds = \int_{-1}^{1} \left(\frac{d}{ds}H_i(\gamma(s))\right) ds = H_i(\nu) - H_i(\mu). \tag{7.1}$$

On the other hand, using the definition of a path integral and the above representation of γ, Equation (7.1) can be furthermore expressed by

$$\int_\gamma h_i(\omega)d\omega = \int_{-1}^{1} h_i(\gamma(s))\gamma'(s)ds = \frac{\nu-\mu}{2}\int_{-1}^{1} h_i\left(\frac{(\mu+\nu)+s(\nu-\mu)}{2}\right) ds. \tag{7.2}$$

Hence, for fixed $\mu = z_0$ and variable $\nu = z$ with $z_0, z \in \mathcal{U}$, $\Psi(z) : \mathcal{U} \to \mathbb{R}^3$

$$\begin{cases} \Psi_1(z) &= Re\left(\frac{z-z_0}{2}\int_{-1}^{1} h_1\left(\frac{(z_0+z)+s(z-z_0)}{2}\right) ds + H_1(z_0)\right) \\ \Psi_2(z) &= Re\left(\frac{z-z_0}{2}\int_{-1}^{1} h_2\left(\frac{(z_0+z)+s(z-z_0)}{2}\right) ds + H_2(z_0)\right) \\ \Psi_3(z) &= Re\left(\frac{z-z_0}{2}\int_{-1}^{1} h_3\left(\frac{(z_0+z)+s(z-z_0)}{2}\right) ds + H_3(z_0)\right), \end{cases} \tag{7.3}$$

yields a representation of the constructed (minimal) surface with translation $Re(H(z_0))$ in $\mathbb{R}^3$.

7.1 Gauss-Kronrod Quadrature

In order to calculate Equation (7.3), a Gauss-Kronrod quadrature is used, which is suitable for an adaptive method and hence, expandable to meromorphic functions with unknown singularities.

Let $a, b \in \mathbb{R}$ and $I(f)$ denote the exact value of integral between a and b

$$I(f) = \int_a^b f(x)dx.$$

Further, let

$$G^{(n)}(f) = \sum_{i=1}^{n} f(x_i)\omega_i$$

be the Gaussian quadrature rule with nodes $a < x_1 < \cdots < x_n < b$ and weights ω_i, $i = 1, \ldots, n$. Then

$$K^{(2n+1)}(f) = \sum_{i=1}^{2n+1} f(\tilde{x}_i)\tilde{\omega}_i \tag{7.4}$$

is called a Gauss-Kronrod quadrature formula [CGGR00, Kro65], if

1. the set of nodes $\{x_i\}_{i=1}^{n}$ is contained in $\{\tilde{x}_i\}_{i=1}^{2n+1}$ and
2. $K^{(2n+1)}(p) = I(p)$ for all polynomials p of degree $3n+1$, i.e., all polynomials of degree less or equal than $3n + 1$ are integrated exact.

Regarding Enumeration (1) function evaluations of f at n points can be reused for the calculation of $K^{(2n+1)}(f)$. Thus, the Gauss-Kronrod formula is applicable for an adaptive implementation, i.e., applying quadrature rules on adaptively refined subintervals, in order to approximate $I(f)$. Note that an adaptive procedure is highly recommended for integrands resp. function evaluations near singularities in order to ensure convergence [PW05].

Usually the difference of the evaluation on Gauss and Kronrod points, i.e.,

$$Err = |G^{(n)}(f) - K^{(2n+1)}(f)|, \tag{7.5}$$

is used as an approximated error [CGGR00].

7.2 Meromorphic Functions

Example 12 in Section 6.1, indicated that an extension to meromorphic functions h is reasonable. As long as the integrands h_i, $i = 1, \ldots, 3$, are holomorphic in a small ϵ-neighborhood around the straight line connecting z with z_0, Equation (7.3) remains well-defined. Though we need to avoid evaluations of h_i, $i = 1, \ldots, 3$, at singularities. The advantage of an adaptive method is that in this case the integral does not converge, a warning can be displayed and the corresponding grid point collinear to a pole and z_0 can

be removed or z_0 be adjusted. Note, since $\mathcal{U}$ contains poles the integral depends on γ and only homotopic paths yield the same result.

As a first example, we make use of the adaptive integration in order to visualize a deformation of a catenoid along the conic section with the plane spanned by two Enneper's minimal curves.

Example 19. *In Equation (6.7) consider $\psi_1 = cat(z)$ a catenoid, $\psi_2 = Enn_3$ and $\psi_3 = Enn_4$ with parameters $\alpha = 100$ as well as $\beta = 2$. Algorithm 1 describes the general construction using a triangulated mesh and Gauss-Kronrod quadrature. The corresponding surfaces are illustrated in Figure 7.1.*

We further visualize a deformation along our parametrization of a catenoid into Enneper's minimal surface of degree 3.

Example 20. *Let again $\psi_1 = cat(z)$ be a catenoid, $\psi_2 = Enn_3$ and fix $\tilde{\Psi}_3 = (1, 2, 1, 0)$ as some point in projective space $\mathcal{P}^3$ in Equation (6.7) and Equation (6.8). The parameters α and β with values between $[0, 100]$ are varied. We use an adaptive Gauss-Kronrod quadrature with an error tolerance of $1e-4$ and a maximum of 50 iterations. The initial value $z_0 = 1 + 1.2i$ was chosen arbitrarily. Figure 7.2 depicts the resulting deformation between a catenoid and Ennerper's surface of degree 3 in the neighborhood $[-\pi : \pi] \times [-\pi : \pi]$, evaluated on a triangulated grid that was created with the `triangle` library. No points had to be removed from the initial triangulation. The procedure converged on all grid points.*

Algorithm 1 Numerical construction of new minimal surfaces

Require: Three minimal curves ψ_1, ψ_2, ψ_3, parameters α, β and definition of a parameter domain $\mathcal{U} = [a : b] \times [c : d]$

$\tilde{\psi}_1 \leftarrow (1, \psi_1')$ ▷ Homogeneous coord.
$\tilde{\psi}_2 \leftarrow (1, \psi_2')$
$\tilde{\psi}_3 \leftarrow (1, \psi_3')$
$cs(\alpha, \beta) \leftarrow \frac{\alpha^2 \langle \tilde{\psi}_1, \tilde{\psi}_3 \rangle_{\mathcal{P}^3} \tilde{\psi}_1 + \alpha\beta\left(\langle \tilde{\psi}_2, \tilde{\psi}_3 \rangle_{\mathcal{P}^3} \tilde{\psi}_1 + \langle \tilde{\psi}_1, \tilde{\psi}_3 \rangle_{\mathcal{P}^3} \tilde{\psi}_2 - \langle \tilde{\psi}_1, \tilde{\psi}_2 \rangle_{\mathcal{P}^3} \tilde{\psi}_3\right) + \beta^2 \langle \tilde{\psi}_2, \tilde{\psi}_3 \rangle_{\mathcal{P}^3} \tilde{\psi}_2}{\alpha \langle \tilde{\psi}_1, \tilde{\psi}_3 \rangle_{\mathcal{P}^3} + \beta \langle \tilde{\psi}_2, \tilde{\psi}_3 \rangle_{\mathcal{P}^3}}$
$h(z) = 1/cs(\alpha, \beta)[0]\,(cs(\alpha, \beta)[1], cs(\alpha, \beta)[2], cs(\alpha, \beta)[3])$ ▷ Define h as a function of z
$area\_pts \leftarrow ((a, c), (b, c), (b, d), (a, d))$ ▷ Specify area for triangulation
$area\_seg \leftarrow ((0, 1), (1, 2), (2, 3), (3, 0))$
$tri \leftarrow tri\_mesh(area\_pts, area\_seg)$ ▷ Generate a triangulated mesh, cf. Listing 10.1
$z_0 \leftarrow r + Is$ ▷ Choose some arbitrary complex value
for $j = 0..2$ **do**
  for $i = 0..length(tri['vertices'])$ **do**
    $int[j] \leftarrow adaptive\_quad(h[j], z_0, tri['vertices'][i][0] + tri['vertices'][i][1] * 1I)$
  end for
end for
return $real(int)$

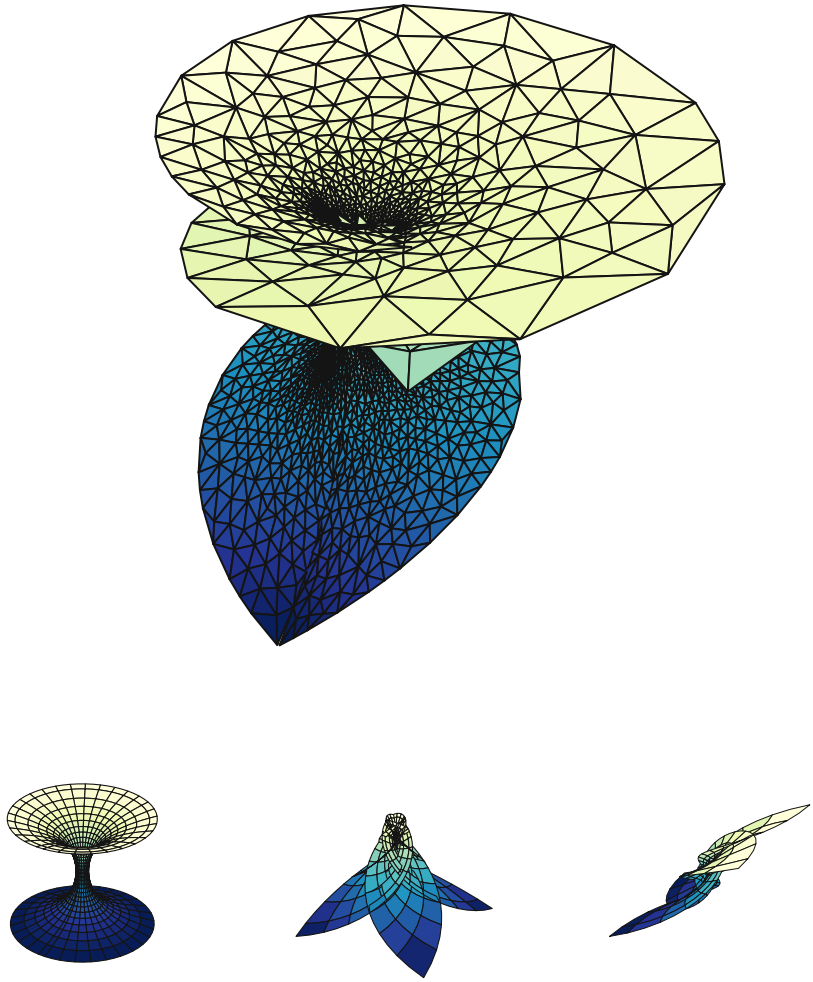

Figure 7.1: Deformed catenoid using $\psi_1 = cat(z), \psi_2 = Enn_3$ and $\psi_3 = Enn_4$ with parameters $\alpha = 100, \beta = 2$ in the domain $[-\pi : \pi] \times [-\pi : \pi]$ evaluated on a triangulated grid with an adaptive method.

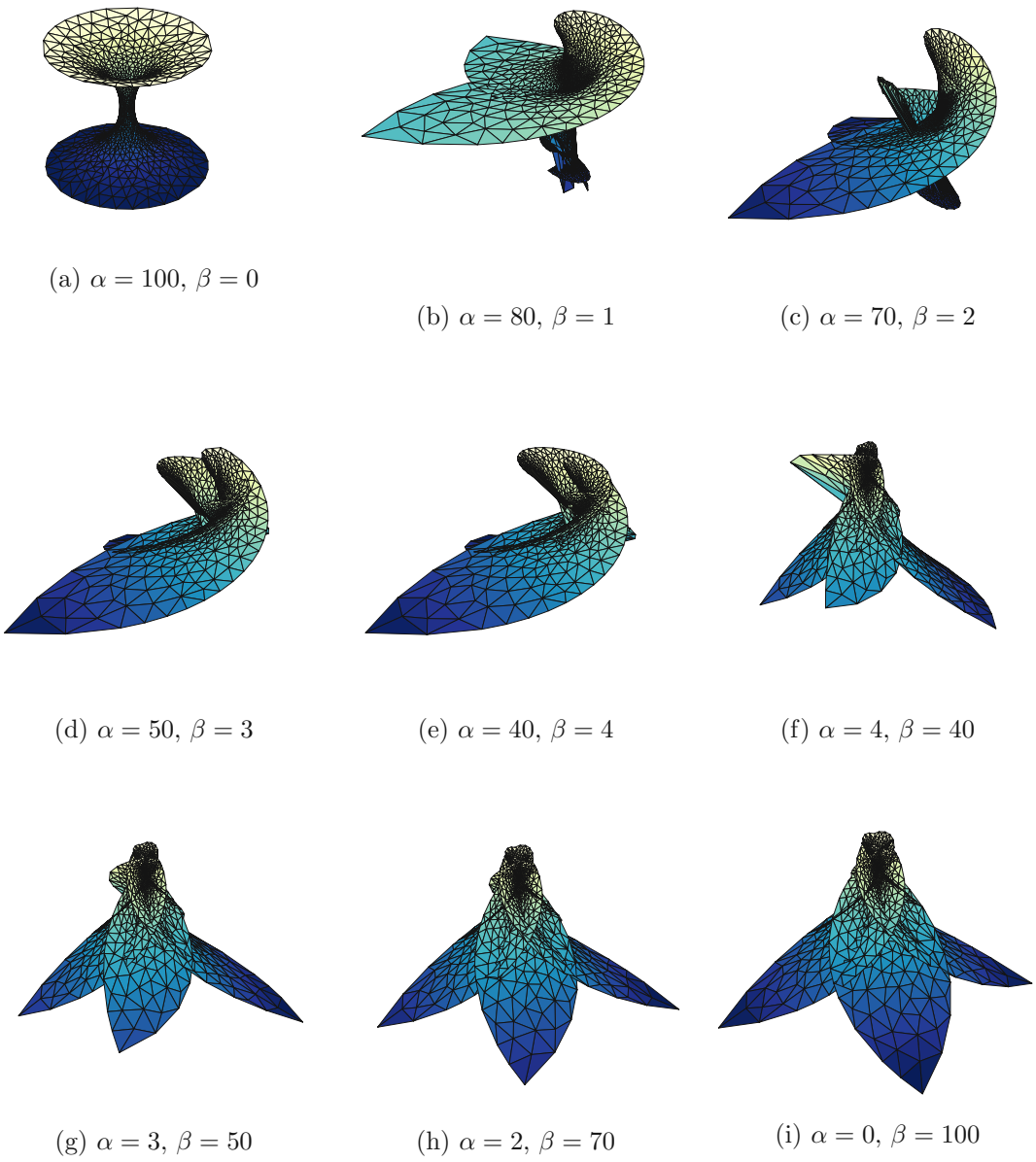

(a) $\alpha = 100$, $\beta = 0$ (b) $\alpha = 80$, $\beta = 1$ (c) $\alpha = 70$, $\beta = 2$

(d) $\alpha = 50$, $\beta = 3$ (e) $\alpha = 40$, $\beta = 4$ (f) $\alpha = 4$, $\beta = 40$

(g) $\alpha = 3$, $\beta = 50$ (h) $\alpha = 2$, $\beta = 70$ (i) $\alpha = 0$, $\beta = 100$

Figure 7.2: Deformation of a catenoid to an Enneper's surface of degree 3. The parameters α and β are in the range $[0, 100]$ and different stepsizes.

8 Christoffel Duality

A further method for constructing minimal surfaces, described in [HJ03, Chapter 5], is based on Christoffel transformation. More specifically, the Christoffel transformation of any isothermic parametrization of a surface is a minimal surface, cf., Theorem 18.

Definition 23. *An isothermic parametrization of a surface is a mapping $f : \mathbb{R}^2 \to \mathbb{R}^3$ such that the partial derivatives of f are orthogonal, $f_u \perp f_v$, conformal, $||f_u|| = ||f_v||$ and conjugate, $f_{uv} \in span\{f_u, f_v\}$ [BS08, Ch. 1.7].*

Example 21. *Let $h : \mathbb{C} \to \mathbb{C}$ be a holomorphic function and σ denote the stereographic projection,*

$$\sigma(z) = \frac{1}{|z|^2 + 1} \left(2Re(z), 2Im(z), |z|^2 - 1\right).$$

Then the composition $\sigma \circ h(z)$ is an isothermic parametrization of the unit sphere S^2 [GAS17, Chapter 8,22].

Theorem 17. *Let $f : \mathbb{R}^2 \to \mathbb{R}^3$ be an isothermic parametrization, then $f^* : \mathbb{R}^2 \to \mathbb{R}^3$, where*

$$f_u^* = \frac{f_u}{||f_u||^2}, \quad f_v^* = -\frac{f_v}{||f_v||^2}, \tag{8.1}$$

is isothermic [BS08, Ch. 1.7].

Definition 24. *The function f^* in Theorem 17, which is unique up to translation, is called the Christoffel transformation or Christoffel dual of f [BS08, Ch. 1.7].*

Theorem 18. *Let $f : \mathbb{R}^2 \to \mathcal{S}^2$ be an isothermic parametrization, then the Christoffel transformation of f^* is a minimal surface [HJ03, Ch. 5.2].*

Since the stereographic projection $g := \sigma \circ h(z)$ of any arbitrary holomorphic function h is an isothermic parametrization, the Christoffel transformation of g yields a minimal surface due to Theorem 18.

Definition 25. *A Möbius transformation is a mapping $m : \mathbb{C} \cup \infty \to \mathbb{C} \cup \infty$ of the form*

$$m : z \mapsto \frac{az + b}{cz + d} \tag{8.2}$$

such that $ad - bc \neq 0$, where $a, b, c, d \in \mathbb{C}$ [Jän13, Ch.10].

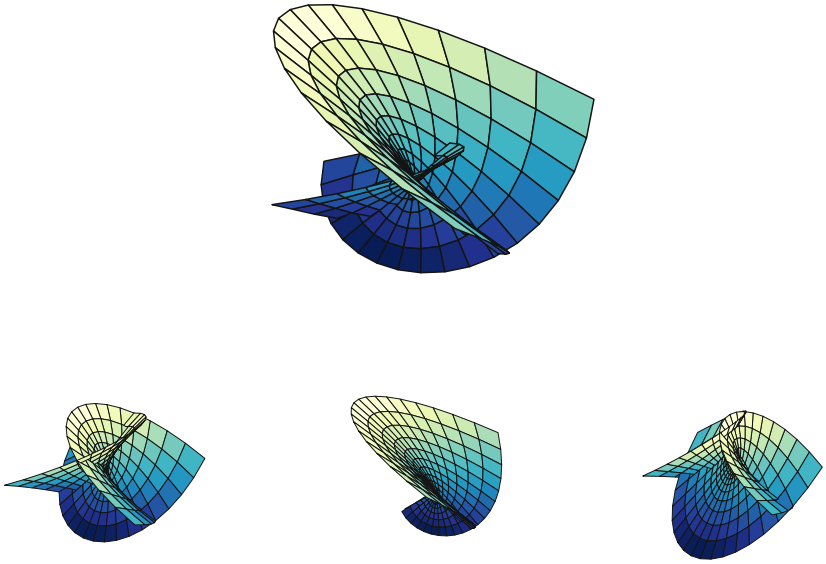

Figure 8.1: Above is the resulting figure after conic section, cf. Equation (6.7) with the parameters $\alpha = \beta = 1$ and the three minimal curves (below) obtained via Christoffel transformation.

Example 22. *Consider the holomorphic function* $f_1(z) := z$ *and the composition of* $f_1(z)$ *with the two Möbius transformation* $m_1(z) = 20z$ *as well as* $m_2(z) = 10z + 10$, *i.e.,* $f_2(z) := m_1 \circ f_1$ *and* $f_3(z) := m_2 \circ f_1$. *As a composition of holomorphic functions, both are holomorphic and by the above remark the Christoffel transformations of the isothermic parametrization* $g_i := \sigma \circ f_i$, $i = 1, 2, 3$ *are minimal surfaces. With* $\psi_i = g_i^*$, $i = 1, 2, 3$ *in Equation (6.7), where the functions* g_i^* *are reconstructed from its known gradient* $(\partial_u g_i^*, \partial_v g_i^*)$, *and parameter* $\alpha = \beta = 1$ *the following algebraic surface, cf. Figure 8.1, is obtained.*

9 3D Printing & Fabrication

The following example is used to produce a 3D printing of a surface obtained by the procedure described in Chapter 6.

Example 23. *Let* $\psi_1 = Enn_5, \psi_2 = Enn_1$ *and* $\psi_3 = Enn_3$ *in Equation (6.7) resp. Equation (6.8) with parameter* $\alpha = 3$ *and* $\beta = 4$ *is considered in a neighborhood* $[-1:1]\times[-1:1]$*, cf. Figure 9.3a-9.3c. We choose a regular* $m \times m$*-grid with* $m = 200$ *supporting points in the complex plane in order to approximate the surface represented by* $Re\left(\int h\right)$*, cf. Figure 9.3d. So, for each grid point we receive an* x, y *and* z *component of* $\mathbb{R}^3$*, in particular there are three* $m \times m$ *matrices, one for each* $\mathbb{R}^3$*-component.*

The surface is exported from Python as OBJ file format [MB08] and further processed in `Blender` [Hes10]. The OBJ file format is an open, text based and human readable file format for 3D geometry definitions. In the simplest case, an OBJ file consists of vertices (v) and polygonal faces (f) pointing on the vertex indices starting with the value 1. In addition, a list of vertex normals (vn), texture coordinates (vt) and line elements (l) can be specified. A simple OBJ file of a triangulated square in the xz-plane is given in Listing 9.1.

```
# OBJ file
v 0 0 0
v 1 0 0
v 0 0 1
v 1 0 1
f 1 2 3
f 2 3 4
```

Listing 9.1: Simple OBJ file of a triangled square.

The surface created in Example 23 can therefore be exported as a triangulated 3D surface in an OBJ file as described in Algorithm 2.

We further use `Blender` in order to recalculate the vertex normals and extrude the surface to a printable solid. The object is adjusted, sliced and framed by supports using a slicer software that produces a so-called `gcode` containing the guidance data for the 3D printer. A first attempt with the setting 'Support on build plate only' revealed that the printer could not cope with the slope in the middle of the object. Therefore, we used the settings:

- Supports: 'Everywhere',
- 0.2mm QUALITY mode and
- Infill: 100%.

The 3D printed model with supports is displayed in Figure 9.1 and the finial printing after removing the supports in Figure 9.2.

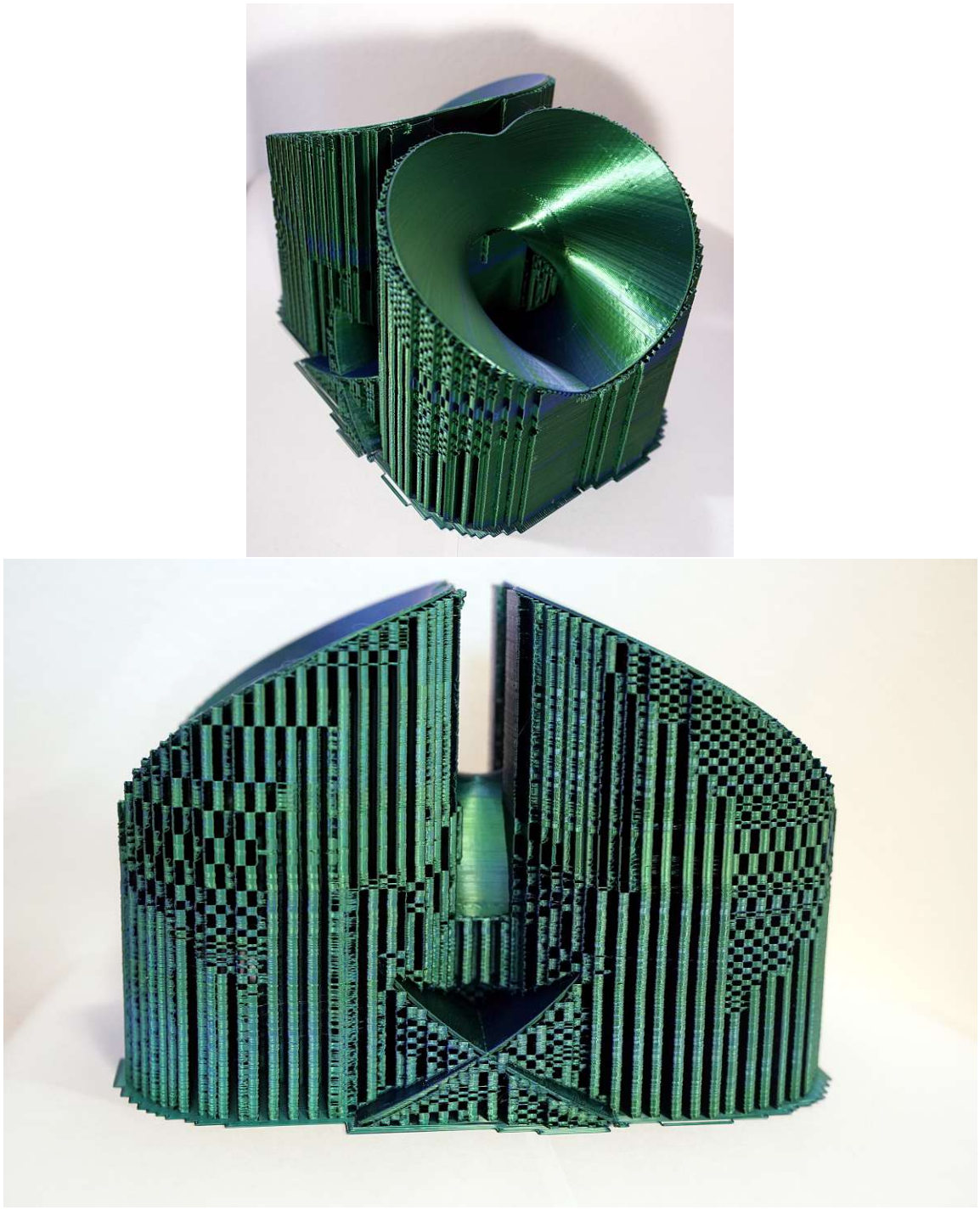

Figure 9.1: 3D printing with supports.

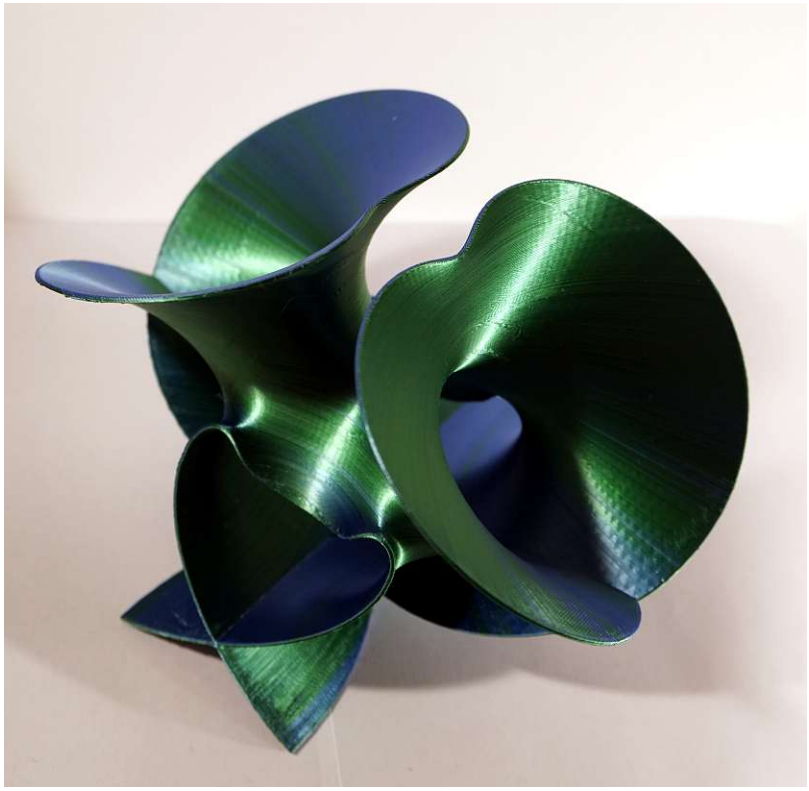

Figure 9.2: 3D printed model with bicolored filament; Enn_5, Enn_1, Enn_3 with $\alpha = 3$, $\beta = 4$ in $[-1:1] \times [-1:1]$.

Algorithm 2 Triangulate grid and store it in OBJ-format

Require: $X, Y, Z \in \mathbb{R}^{m \times m}$ containing x, y, z-coordinates of the surface, G regular $m \times m$ grid

$n \leftarrow m^2$ ▷ Number of grid elements
$xyz \leftarrow zeros((n, 3))$
$xyz[:, 0] \leftarrow reshape(X, -1)$ ▷ Save all x-coordinate to 1st column
$xyz[:, 1] \leftarrow reshape(Y, -1)$
$xyz[:, 2] \leftarrow reshape(Z, -1)$
for $i \leftarrow 0 \ldots n$ **do** ▷ Insert vertices v
    write("v %.6f %.6f %6.f \n" % tuple($xyz[i]$))
end for
for $j \leftarrow 0 \ldots n - m$ **do** ▷ Add faces f
    if $(j + 1)$ modulo m ! $= 0$ **then**
        write("f %d %d %d \n" % tuple($(j + 1, j + 2, m + j + 1)$))
        write("f %d %d %d \n" % tuple($(j + 2, m + j + 1, m + j + 2)$))
    end if
end for

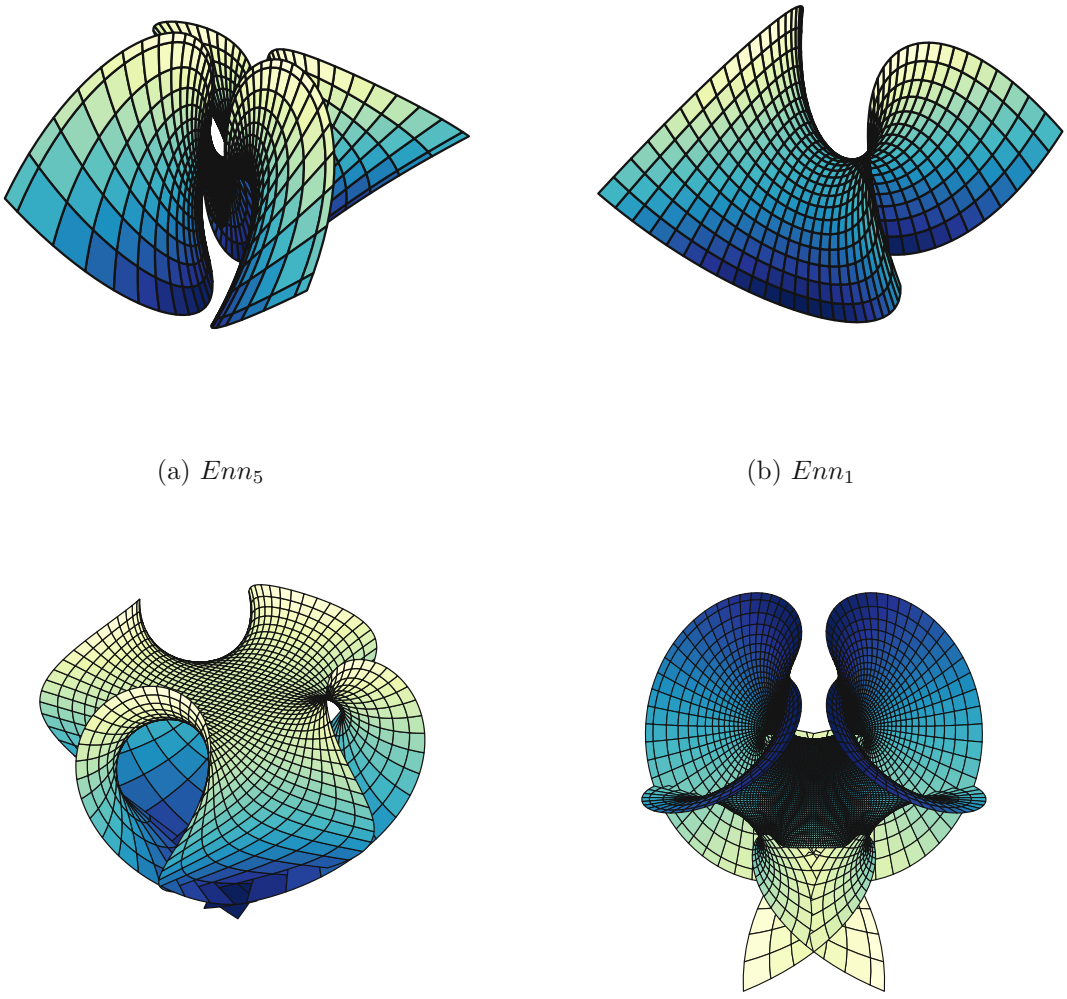

(a) Enn_5 (b) Enn_1

(c) Enn_3 (d) Generated surface

Figure 9.3: Initial minimal surfaces, $\psi_1 = Enn_5$, (a), $\psi_2 = Enn_1$, (b) and $\psi_3 = Enn_3$, (c), in the domain $[-1, 1] \times [-1, 1]$. Resulting 3D model (d).

10 Conclusion & Open Questions

We provided a method to construct new surfaces via the identification of minimal curves as points on a projective quadric and the intersection of this cone with the plane spanned by three different minimal curves, where surfaces of an associated family belong to the rulings of the cone. If only algebraic minimal curves are utilized, in order to build the conic section, locally, outside of an isolated singularity, the generated surface is minimal. It is still open whether this result can be extended to other types of minimal curves. Further, we motivated the use of the obtained parametrization as a deformation formula between minimal surfaces and have generated numerous examples with the procedure described in Chapter 6. Utilizing analytically defined functions in the equation of the conic section was a challenge, regarding the determination of singularities potentially contained in the integrand and it was not possible to determine them with Python built-in functions. In the practical examples, this circumstance has not caused any problems in the presented adaptive integration method. However, this case is still covered by excluding a neighborhood of such points (and those collinear to them) in the triangulation, cf. Listing 10.1. It would be interesting if those isolated singularities are of importance for physics or material science. In the context of 3D printing and from a mathematical point of view, it would be worthy of investigation whether the presented approach could be used to generate periodic minimal surfaces.

Appendix

Theorem 19 (Gaussian divergence theorem)**.** *[For12] Let $\Omega \subseteq \mathbb{R}^n$ be open and bounded such that $\partial\Omega \in C^1$ and let ν denote the outer normal vector on $\partial\Omega$. For $F \in C^0(\bar{\Omega}, \mathbb{R}^n) \cap C^1(\Omega, \mathbb{R}^n)$ and let $\operatorname{div} F$ be integrable on Ω then*

$$\int_\Omega \operatorname{div} F \, dx = \int_{\partial\Omega} \langle F, \nu \rangle \, ds. \tag{10.1}$$

Further, consider a compact topological space $(X, \mathcal{T})$.

Definition 26. *A subset F of continuous, bounded functions $f : X \to \mathbb{R}$ $(\mathbb{C})$, $\mathcal{C}_b(X, \mathbb{R})$, is **pointwise bounded**, if $\sup_{f\in F} |f(x)|$ is bounded for all $x \in X$ [Kal15].*

Definition 27. *A set $F \subseteq \mathcal{C}_b(X, \mathbb{R})$ $(\mathcal{C}_b(X, \mathbb{C}))$ is called **equicontinuous**, if for each $x \in X$ and for every $\epsilon > 0$ it holds that $|f(y) - f(x)| < \epsilon$ for all $y \in X$ with $|x - y| < \delta$ and for all $f \in F$ [Kal15].*

Theorem 20 (Arzelà Ascoli)**.** *Let $(X, \mathcal{T})$ be a compact topological space and $F \subseteq \mathcal{C}_b(X, \mathbb{R})$ $(\mathcal{C}_b(X, \mathbb{C}))$. Then F is pointwise bounded and equicontinuous if and only if the closure of F, denoted by $\bar{F}$, is compact. In particular, every sequence in F has a uniformly convergent subsequence [Kal15].*

Generally known sum-to-product identities for trigonometric functions:

$$\cos(\alpha) + \cos(\beta) = 2\cos\left(\frac{\alpha-\beta}{2}\right)\cos\left(\frac{\alpha+\beta}{2}\right) \tag{10.2}$$

$$\sin(\alpha) + \sin(\beta) = 2\cos\left(\frac{\alpha-\beta}{2}\right)\sin\left(\frac{\alpha+\beta}{den}\right). \tag{10.3}$$

In Listing 10.1 we provide Python code using the `triangle` library for a triangulation with the possibility to exclude circular neighborhoods around poles.

Further, we provide a visualization of the deformation from Enneper's minimal surface Enn_1 over Enn_2, Enn_3 to Enn_4, cf. Figure 10.1, Figure 10.2 and Figure 10.3.

```
def tri_mesh(area_points, area_seg, poles, R=0.1, tr_ref=0.01):
        """
        Parameters
        ----------
        area_points : darray
                Define the area to be triangulated.
        area_seg : darray
                Corresponing segments required in order to describe the area
                    that needs to be triangulated.
        poles : list
                List containing poles / points, where the mesh should have
                    holes.
        R : float
                Radius of holes in the mesh.
        tr_ref : float
                Refers to the area of a triangle, i.e., no triangle has area
                    greater than R, cf. 'triangle.triangulate()'.
        *z0= : complex
                Point in the complex plane.
        Returns
        -------
        A triangulated mesh. Unless the list of poles is not empty the mesh
            leaves out circular holes.
        """
        tr_type = 'qpa'+str(tr_ref)
        if len(poles)==0:
                T = dict(vertices=area_points, segments=area_seg)
                ret = tr.triangulate(T, tr_type)
                tr.compare(plt, T, ret)
                plt.show()
        else:
                N = 9
                theta = np.arange(N) * 2 * np.pi / N
                mesh_holes = [[np.real(k), np.imag(k)] for k in poles]
                pts = area_points
                seg = area_seg
                for k in range(0,len(poles)):
                        pts = np.vstack([pts,np.stack([mesh_holes[k][0]+R*np.
                            cos(theta), mesh_holes[k][1]+R*np.sin(theta)],
                            axis=1)])
                        tmp = np.stack([np.arange(N), np.arange(N)+1], axis
                            =1) % N
                        seg = np.vstack([seg, tmp + seg.shape[0]])
                T = dict(vertices=pts, segments=seg, holes=mesh_holes)
                ret = tr.triangulate(T, tr_type)
                tr.compare(plt, T, ret)
                plt.show()
        return ret
```

Listing 10.1: Triangulation with Python using the `triangle` library.

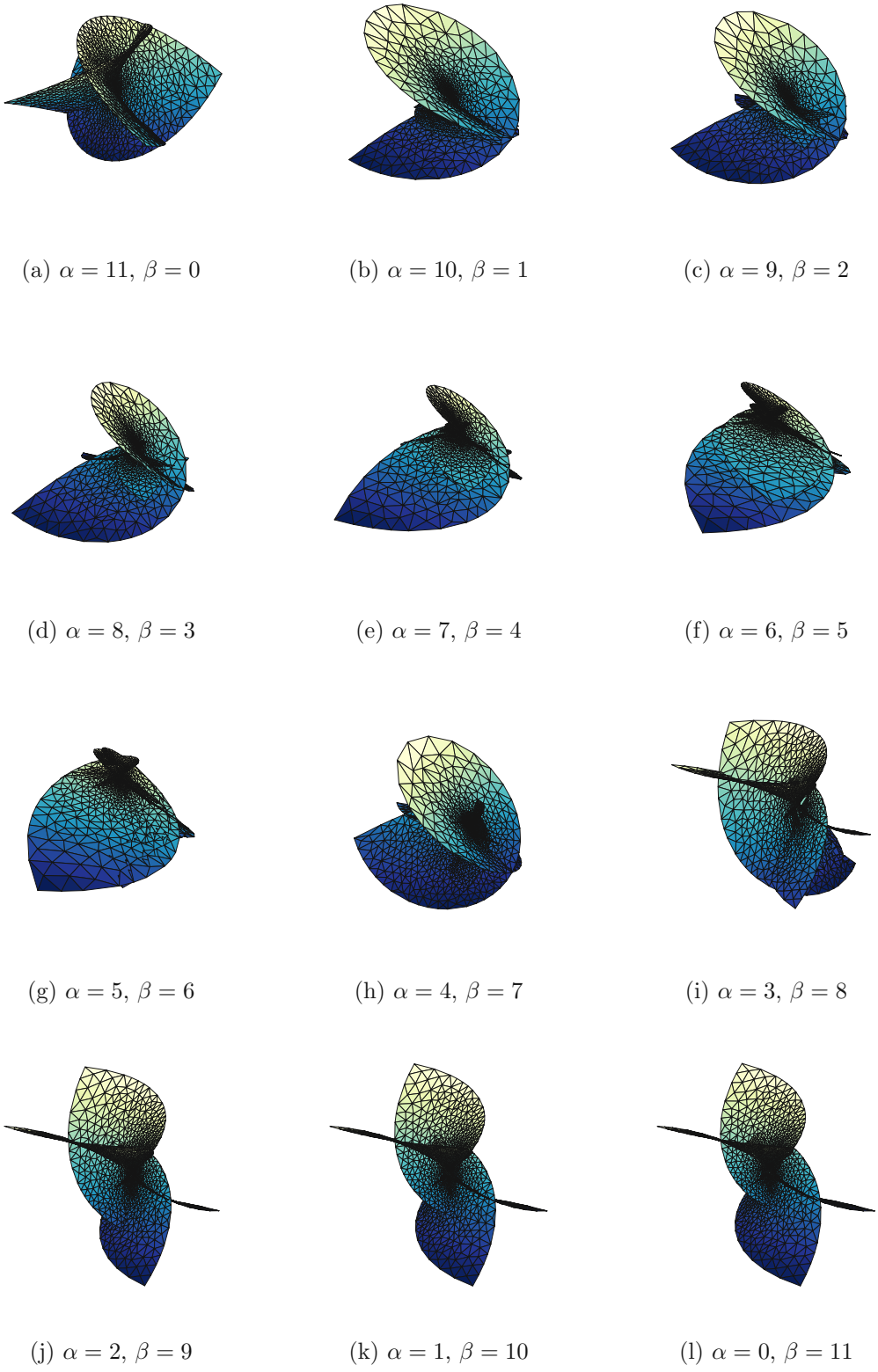

(a) $\alpha = 11$, $\beta = 0$ (b) $\alpha = 10$, $\beta = 1$ (c) $\alpha = 9$, $\beta = 2$

(d) $\alpha = 8$, $\beta = 3$ (e) $\alpha = 7$, $\beta = 4$ (f) $\alpha = 6$, $\beta = 5$

(g) $\alpha = 5$, $\beta = 6$ (h) $\alpha = 4$, $\beta = 7$ (i) $\alpha = 3$, $\beta = 8$

(j) $\alpha = 2$, $\beta = 9$ (k) $\alpha = 1$, $\beta = 10$ (l) $\alpha = 0$, $\beta = 11$

Figure 10.1: Deformation Enneper's surface of degree 1 to 2; fixed point $(1, 1, 0, 0)$.

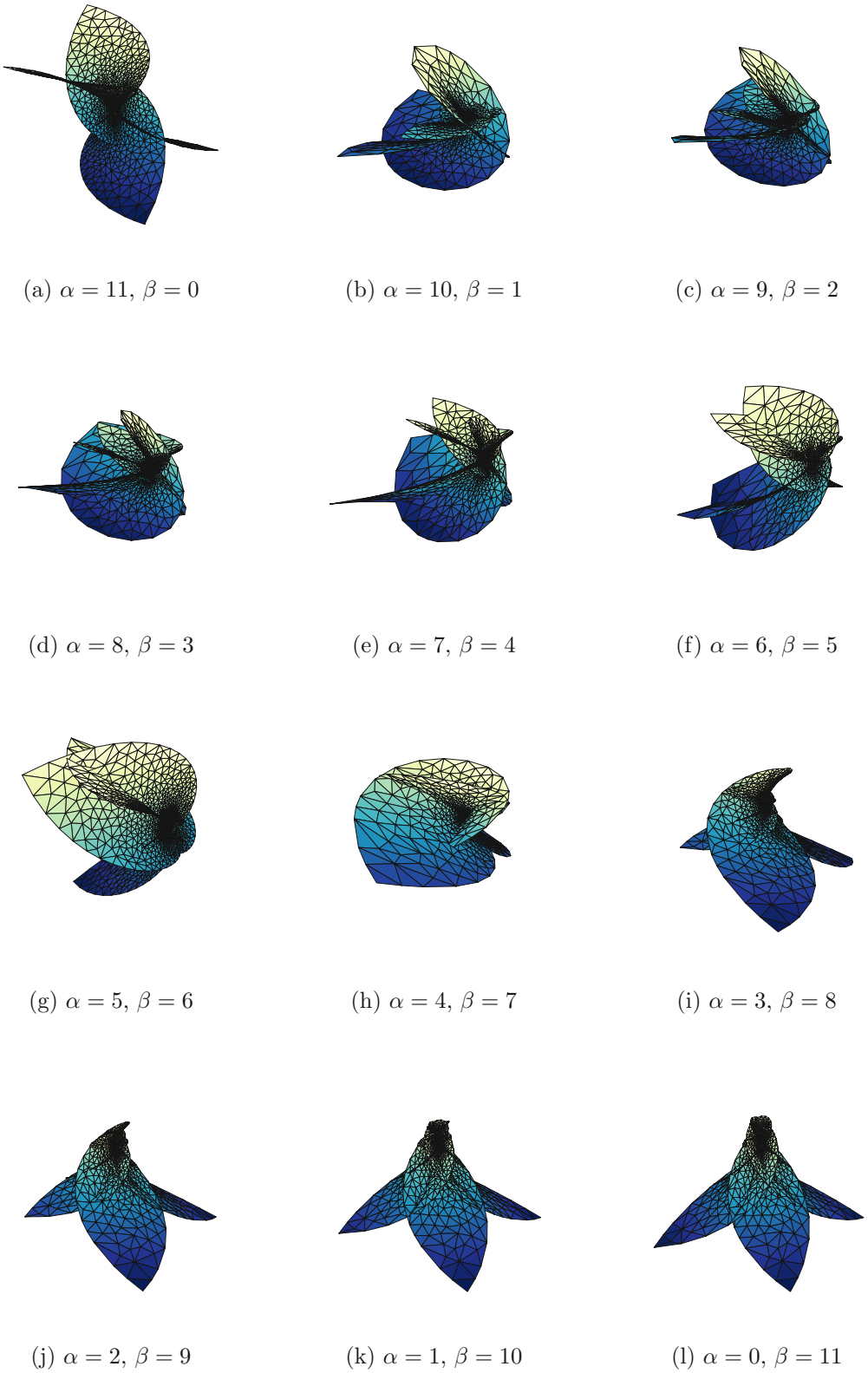

(a) $\alpha = 11, \beta = 0$ (b) $\alpha = 10, \beta = 1$ (c) $\alpha = 9, \beta = 2$

(d) $\alpha = 8, \beta = 3$ (e) $\alpha = 7, \beta = 4$ (f) $\alpha = 6, \beta = 5$

(g) $\alpha = 5, \beta = 6$ (h) $\alpha = 4, \beta = 7$ (i) $\alpha = 3, \beta = 8$

(j) $\alpha = 2, \beta = 9$ (k) $\alpha = 1, \beta = 10$ (l) $\alpha = 0, \beta = 11$

Figure 10.2: Deformation Enneper's surface of degree 2 to 3; fixed point $(1, 1, 0, 0)$.

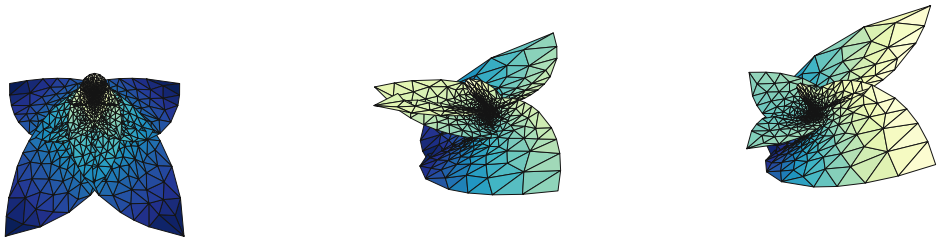

(a) $\alpha = 11$, $\beta = 0$ (b) $\alpha = 10$, $\beta = 1$ (c) $\alpha = 9$, $\beta = 2$

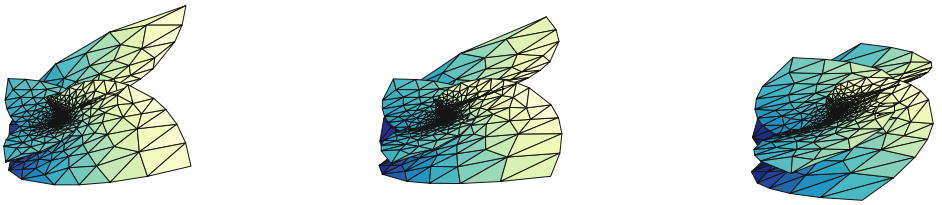

(d) $\alpha = 8$, $\beta = 3$ (e) $\alpha = 7$, $\beta = 4$ (f) $\alpha = 6$, $\beta = 5$

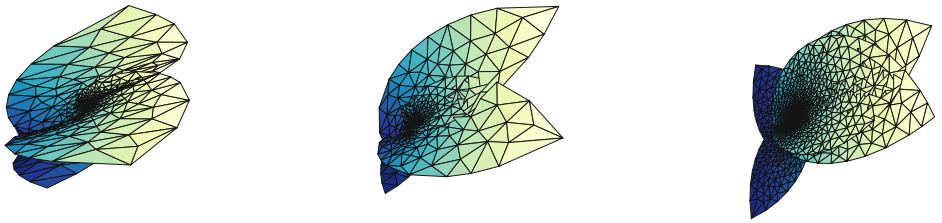

(g) $\alpha = 5$, $\beta = 6$ (h) $\alpha = 4$, $\beta = 7$ (i) $\alpha = 3$, $\beta = 8$

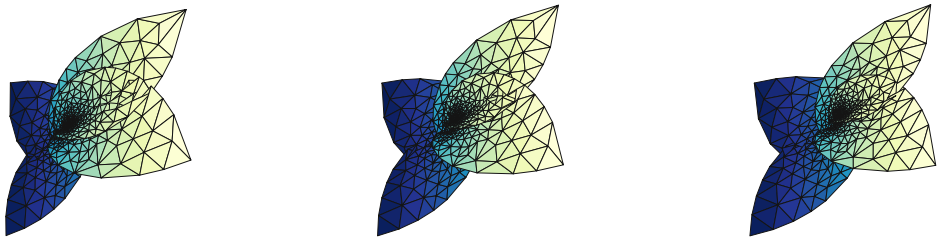

(j) $\alpha = 2$, $\beta = 9$ (k) $\alpha = 1$, $\beta = 10$ (l) $\alpha = 0$, $\beta = 11$

Figure 10.3: Deformation Enneper's surface of degree 3 to 4; fixed point $(1, 1, 0, 0)$.

List of Figures

Bibliography

[AH+84] Sten Andersson, S. T. Hyde, et al. The intrinsic curvature of solids. *Zeitschrift für Kristallographie-Crystalline Materials*, 168(1-4):1–18, 1984.

[Bjö44] Emanuel G. Björling. In integrationem aequationis derivatarum partialum superfici, cujus in puncto unoquoque principales ambo radii curvedinis aequales sunt sngoque contrario. *Arch. Math. Phys*, 4(1):290–315, 1844.

[BS08] Alexander I. Bobenko and Yuri B. Suris. *Discrete Differential Geometry: Integrable Structure*. American Mathematical Soc., 2008.

[CGGR00] Daniela Calvetti, Gene H. Golub, Willian Gragg, and Lothar Reichel. Computation of Gauss-Kronrod quadrature rules. *Mathematics of computation*, 69(231):1035–1052, 2000.

[Cou37] Richard Courant. Plateau's problem and Dirichlet's principle. *Annals of Mathematics*, 38(3):679–724, 1937.

[DC86] Manfredo P. Do Carmo. The helicoid. In *Mathematical Models from the Collections of Universities and Museums*, pages 44–45. Vieweg, Braunschweig, 1986.

[Dou31] Jesse Douglas. Solution of the problem of Plateau. *Transactions of the American Mathematical Society*, 33(1):263–321, 1931.

[EJ14] Jost-Hinrich Eschenburg and Jürgen Jost. *Differentialgeometrie und Minimalflächen*. Springer-Verlag, 2014.

[Emm13] Michele Emmer. Minimal surfaces and architecture: New forms. *Nexus Network Journal*, 15(2):227, 2013.

[Enn68] Alfred Enneper. Analytisch-geometrische Untersuchungen. *Nachrichten von der Königl. Gesellschaft der Wissenschaften und der Georg-Augusts-Universität zu Göttingen*, 1868:421–443, 1868.

[Eul52] Leonhard Euler. *Methodus inveniendi lineas curvas maximi minimive proprietate gaudentes sive solutio problematis isoperimetrici latissimo sensu accepti*, volume 1. Springer Science & Business Media, 1952.

[For12] Otto Forster. *Analysis 3: Maß-und Integrationstheorie, Integralsätze im $\mathbb{R}^n$ und Anwendungen*. Springer Science & Business Media, 2012.

[GAS17] Alfred Gray, Elsa Abbena, and Simon Salamon. *Modern differential geometry of curves and surfaces with Mathematica®*. Chapman and Hall/CRC, 2017.

[Hen75] Lebrecht Henneberg. *Über solche Minimalflächen, welche eine vorgeschriebene ebene Curve zur geodätischen Linie haben.* Dissertation, Zürich, 1875.

[Hen76] Lebrecht Henneberg. Über diejenige Minimalfläche, welche die Neilsche Parabel zur ebenen geodätischen Linie hat. *Wolf Z*, 21:17–21, 1876.

[Hes10] Roland Hess. *Blender Foundations : The Essential Guide to Learning Blender 2.6.* Boston : Focal Press, 2010.

[HJ03] Udo Hertrich-Jeromin. *Introduction to Möbius differential geometry.* Cambridge University Press, 2003.

[Jän13] Klaus Jänich. *Funktionentheorie: Eine Einführung.* Springer-Verlag, 2013.

[Kal15] Michael Kaltenbäck. *Fundament Analysis.* Heldermann Verlag, 2015.

[Kro65] Alexander Kronrod. Nodes and weights of quadrature formulas: sixteen-place tables. consultants bureau, 1965.

[Küh15] Wolfgang Kühnel. *Differential geometry*, volume 77. American Mathematical Soc., 2015.

[Lag60] Joseph-Louis Lagrange. Essai dune nouvelle methods pour deteminer les maxima et les minima. *Misc. Taur.*, 2:356–357, 1760.

[Lie22] Sophus Lie. Gesammelte Abhandlungen, Vol. 1–6. *Leipzig, Teubner (1922–1937)*, 1922.

[LM83] William Longley and Thomas McIntosh. A bicontinuous tetrahedral structure in a liquid-crystalline lipid. *Nature*, 303(5918):612–614, 1983.

[MB08] Kenton McHenry and Peter Bajcsy. An overview of 3D data content, file formats and viewers. *National Center for Supercomputing Applications*, 1205:22, 2008.

[Meu85] Jean Baptiste Meusnier. Mémoire sur la courbure des surfaces. *Mem des savan etrangers*, 10(1776):477–510, 1785.

[Mül20] Christian Müller. *Vorlesungsnotizen Projektive Geometrie.* 2020.

[Nit89] Johannes C Nitsche. *Lectures on minimal surfaces.* Cambridge University Press, 1989.

[Ode16] Boris Odehnal. On algebraic minimal surfaces. *KoG*, 20(20):61–78, 2016.

[Oss70] Robert Osserman. A proof of the regularity everywhere of the classical solution to Plateau's problem. *Annals of Mathematics*, pages 550–569, 1970.

[PW01] Helmut Pottmann and Johannes Wallner. *Computational Line Geometry.* Springer, 2001.

[PW05] Leszek Plaskota and Grzegorz W. Wasilkowski. Adaption allows efficient integration of functions with unknown singularities. *Numerische Mathematik*, 102(1):123–144, 2005.

[Rad30] Tibor Radó. On Plateau's problem. *Annals of Mathematics*, pages 457–469, 1930.

[Sch70] Alan H. Schoen. Infinite periodic minimal surfaces without self-intersections. Technical report, 1970.

[She22] Shafaq Naz Sheikh. The Theory of Minimal Surfaces in $\mathbb{R}^3$ with a look at the Area Minimizing Property. Master's thesis, 2022.

[SKO20] V. Ya. Shevchenko, M. V. Kovalchuk, and A. S. Oryschenko. Synthesis of a new class of materials with a regular (periodic) interconnected microstructure. *Israel journal of chemistry*, 60(5-6):519–526, 2020.

[Wei66] Karl Weierstrass. *Untersuchungen über die Flächen, deren mittlere Krümmung überall gleich Null ist*. Königl. Akademie der Wissenschaften zu Berlin, 1866.